CHAPTER 5

Properties of Palm Oil Emulsions Prepared using Emuldan

5.1 Introduction

A whole range of synthetic and natural emulsifiers are available in the market but generally food emulsifiers are derived from natural organic products such as vegetable oils (mainly soyabean and palm oils), animal fats (mainly lard and tallow) and glycerol. From these raw materials, fatty acids and monoglycerides are made. Purified, distilled monoglycerides are used in various edible products such as bread (1), bakery products (2), oil-in-water emulsions for whipped creams (3) and sausages (4). Further derivitisation of monoglycerides with organic acids such as lactic, citric, tartaric or acetic acids results in a wide range of food acid esters of monoglycerides which are important commercial food emulsifiers too (5).

Functionally, food emulsifiers are used to reduce the interfacial tension at the oil-water interface, thus promoting emulsification and heterogeneous phase formation. Due to its surface active properties,

emulsifiers have also been used indirectly in textural and rheological modifications.

Many food grade emulsifiers are available commercially for the possible emulsification of palm oil. To narrow down their selection and to achieve the objective of producing more value added products from palm oil, a range of vegetable oil derived emulsifiers was screened (6). A commercial emulsifier, Emuldan 50/S2 (commercially specified as a mixture of mono and diglycerides consisting of at least 50% monoester and 2% sodium stearate) was found to show interesting behaviour with respect to emulsion droplet size and viscosity. An added interest in such mixtures of monoglycerides is that relatively pure monoglycerides have been synthesized using palm stearin as the raw material (7) while large scale commercial productions of monoglycerides are also available utilising vegetable oils including palm oil and its products (8).

In view of the wide scope of possible utilisation of emulsified vegetable oil in products ranging from very dilute emulsions as in parenteral preparations (9) to low and medium concentration of oil in the more recent novel fat spread (10) and high oil phase volume products like mayonnaise (11) and margarine (12), the task of selecting the most appropriate concentration range for the major components of an emulsion: namely emulsifier, water and

oil, can be an extremely complicated practical problem. Thus in order to characterise the behaviour of such a complex lipid mixture, an attempt was made to determine the ternary diagram of the three components. From a commercial view point, the minimal use of the most expensive component, in the order of emulsifier and oil, that meets the user's requirement shall be the most economically viable.

5.2 Binary Phase System and Liquid Crystalline Phases

Various mesomorphic phases in the binary system of water and monoglycerides have been determined and referred to regularly (13). Some of the structures of liquid crystals in water are illustrated in Fig. 1 (14). The lamellar liquid crystal phase is the most common and it consists of alternate layers of water and bimolecular lipid layers. It can be swollen with water and may have almost infinite swelling capacity if ionised amphiphilic molecules are introduced into the bilayer or if the aqueous phase has a low ion concentration (15,16). Diluted lamellar phases may form liposomes which are spherical aggregates with an internal lamellar structure (17). Other types of mesomorphic phases are the hexagonal and cubic phases. The hexagonal I phase may consist of cylindrical aggregates of surfactant molecules with the polar group oriented towards the (continuous) water phase and the surfactant hydrocarbon chains filling

the core of the cylinder. This hexagonal I phase can be diluted to form spherical micelles. The hexagonal II phase consists of cylindrical aggregates of water in a continuous medium of lipid with the polar groups orientated towards the water phase and the hydrocarbon chains filling out the exterior between the water cylinders. In view of its structural arrangement the hexagonal II phase has limited swelling capacity of about 40% water in the cylindrical aggregates. At high temperature, a viscous isotropic cubic phase can exist in monoglyceride/water system for emulsifiers with chain length longer than C12:0 (13). This behaves as very viscous liquid phase and can also accommodate up to approximately 40% water.

Monoglycerides of various chain lengths (C12-22) and degree of unsaturation form different types of mesophases at different temperatures and water concentrations (13). The dominant mesophase in monopalmitin is the lamellar phase which swells to a maximum of 40% water. When the water concentration is greater than 60%, dispersions are formed at 55-68°C. At temperature higher than 68°C, viscous cubic phase in equilibrium with water is formed (18). A commercial distilled monoglyceride, DGMS, which consists of mainly monostearate and monopalmitin is known to behave similarly to that of monopalmitin with minor changes in the phase diagram (18,19). DGMS with 40% water forms lamellar phase when heated, and in the

transition stage, an α crystalline gel phase is formed (19, see Fig. 1). The gel structure is of the lamellar type as in a lamellar phase. The difference is that the hydrocarbon chains are no longer in liquid-like state but are solid and orientated parallel to each other in an α crystalline mode of packing. X-ray diffraction confirms the α-form chain packing (18). If a small amount of a charged lipid like sodium stearate (0.5% calculated on DGMS) is present, the swelling will proceed to accommodate more water (15, 18). The water layer may be a few hundred angstrom thick. This gel phase is metastable because the water layer between the polar groups may be reduced with time. However, it can take up to a year for it to transform into ß crystals of monostearin and water (cogel) mixture, when all the water is expelled. The transition is delayed by the presence of impurities solubilised into the α layer. It was also found that controlled neutralisation of the free fatty acids, which are always present in commercial monoglycerides, with sodium hydroxide enhances significantly the swelling behaviour of the monoglycerides. The effect is similar to the addition of polar lipid (sodium stearate). The stability of the gel is also sensitive to ion concentration eg. sodium chloride in the water, but is independent of the pH (18).

5.3 Ternary System

Phase diagrams are commonly drawn to illustrate the behaviour of the ternary system at various concentrations of the individual components. They have been used to illustrate the various phases of oil, water and emulsifier together with the various liquid crystalline phases, gel, emulsions and micellar phases which occur in a ternary system (20-26). Ternary diagram has also been applied in the formulation of cosmetics (27). Ternary systems consisting of soyabean oil triglycerides in the liquid state, water and food emulsifier have been described by various workers (20-24). Hemker (20) had identified various liquid crystalline types and crystalline gel of some food-grade polyglycerol ester emulsions with soyabean oil and water. Rydhag (21) reported several phase diagrams involving soybean oil, water and phospholipids of various degrees of purity. In all the phase diagrams, the three phases i.e oil, water and lamellar liquid crystals were in equilibrium, corresponding to the oil-in-water type of emulsion. Lindstrom (22) and Engstrom (23) studied the soyabean oil/sunflower monoglycerides/water system. The main region of the phase diagram contains water and an L2-phase (isotropic solution with reversed micelles where curved lipid bilayers are arranged in parallel, separating aqueous layer of finite size). Various types

of liquid crystals were also identified as the concentrations of the components were varied. Gulik et. al (24) further studied the L2 inverse micellar solution and various liquid crystalline structures by electron microcopy and confirmed the structures proposed by Engstrom (23) through X-ray studies. Hamdan (28) using palm olein identified lamellar liquid crystals at relatively high concentration of surfactants in the palm olein/water/hexanol and cationic surfactant systems.

5.4 Stabilisation of Emulsions

Friberg and coworkers (29) proposed that liquid crystalline phases may stabilise emulsion by forming a film at the oil/water interface. The formation of multilamellar structure at the oil droplet surface in emulsion contributes to droplet stability. Lamellar liquid crystalline phases formed by different ratios of Tween 40 and Span 40 on sunflower oil in water emulsion droplet surface have been identified by electron microscopy (30). Sodium steroyl lactylate and water formed lamellar mesophases with water up to 40 wt % at temperature above 45°C but when triglycerides (soyabean oil) was added the hexagonal II structure was formed (18). This hexagonal structure can solubilise up to 10% oil and 20% water. If more water was added an oil-in-water emulsion was formed, with liquid crystal being

formed at the droplet surface. At high concentration of the emulsifier, the liquid crystalline layers around the oil droplets may be easily identified under the polarising microsope. Unsaturated monoglycerides of monolinoleate formed viscous isotropic, cubic mesophase with water but in the presence of triglycerides, they were tranformed to hexagonal II mesophase. With excess oil, an oil-in-water emulsion was formed with liquid crystalline structure covering the oil droplet surface (18).

Monoglycerides when used singly or in combination with other surfactants such as diglycerides and proteins, can stabilise oil droplets (31,33). The glycerides interact with the proteins and give rise to viscoelastic property of the emulsion, thereby contributing to the droplet stability. Microemulsions of canola oil could be formed with the aid of monoglycerides and an alcohol cosurfactant which increased the mutual solubility of the oil and water (34).

In emulsions, the droplets may be stabilised by the surfactant on the surface but due to density difference creaming may occur, although coalescence is prevented. According to Stoke's Law, the rate of creaming is given by:

$$V = \frac{2G\, r^2\, (d_1 - d_2)}{\eta}$$

where V = Rate of Creaming ($m\ s^{-1}$)

G = Gravitational acceleration ($m\ s^{-2}$)

r = Radius of droplets (m)

d_1, d_2 = Densities of continuous phase and droplet respectively ($kg\ m^{-3}$)

η = Viscosity ($kg\ m^{-1}\ s^{-1}$)

Thus retardation of creaming can be achieved by increasing the viscosity, N, of the medium. This affects the overall rheology of the final product.

5.5 Rheology of Emulsions

An understanding of the flow characteristics or rheology of emulsions is vital in many industrial processing and product formulations. These are food emulsions, cosmetics, paints, agrochemicals, pharmaceuticals, printing inks, adhesives and other industrial and household products. The rheological properties affect the stability, aesthetic value, functionality and applicability of the products. The rheological properties of emulsions may be affected by factors such as the volume fraction of the dispersed phase (35); the interfacial viscosty and elasticity of the dispersed droplets (36); the droplet size distribution (37) and the viscosity and chemical composition of the dispersion medium (38,39).

Other factors which affect the rheology of emulsions relate to the property of the continuous phase which may form a "gel" net-work (40,41). Gel here means a network formation of macromolecules where water is embedded in the matrix which is commonly formed by hydrocolloids in food formulations. These hydrocolloids may form dispersions or adsorb at the oil droplet surface and gave rise to various rheological behaviour (41-44).

The rheology of the liquid crystals of surfactant Aerosol OT has been studied with respect to the low and high regime of AOT concentration in water (45,46). At 25°C and at a concentration range of 1.4-18.5 wt %, biphasic liquid crystals are formed. Below 3 wt % concentration AOT in water, dispersions are formed and they behaved as Newtonian fluid. At higher concentration of 8 wt %, phase inversion takes place where the dispersions changes from being water continuous to liquid crystalline continuous. Between 18.5 ± 1 to 75 wt %, they form lamellar liquid crystalline phases while above 75 wt %, viscous isotropic and hexagonal phases were formed. These structural changes resulted in various rheological changes.

Various rheological viscoelastic models were constructed for the different liquid crystalline phases in the ternary system of water/mineral oil/ether-linked non-ionic surfactant (polyoxyethylene derivative of oleic

alcohol) where a low stress measurements(creep rheometer) distinguished the different phases (47). The viscoelastic properties of sunflower oil emulsions containing specific ratios of Tween/Span were attributed to the formation of a liquid crystalline phase both in the continuous medium and at the surface of the oil droplets (30).

5.5.1 Measurement of Emulsion Rheology

Rheology measurements may be divided into linear and non-linear behaviour regime. The non-linear properties are a function of the applied stress, strain or shear rate where the parameters of importance are the viscosity and possible normal stress difference. The measurements in the linear range include the viscoelastic moduli such as the frequency dependent storage and loss moduli, G' and G" respectively or the various combinations of such complex moduli G* and the phase lag tan δ. In the linear range the time dependent creep compliance is another commonly measured parameter. Generally such measurements are confined to that range of stress or strain below any perceivable visual movements during measurements. They are thus useful in assessing the microstructures or crystalline phases and possibly long term stability of the system.

5.6 Outline of Study

In this study an initial phase diagram of the Emuldan/palm olein/water system was constructed with the objective to identify the region where stable palm olein droplets can be formed in an aqueous medium to produce stable oil-in-water emulsions. Mechanical agitation was applied to the system to homogenise the mixture.

Various mesophases similar to those found in the binary system of pure monoglyceride/water system or ternary system of monoglyceride/triglyceride (vegetable oil)/water were probably present in the Emuldan/olein/water system. The utilisation of palm olein which is a mixture of triglycerides, diglycerides, fatty acids and monoglycerides adds to the complexity of an already complex system of emulsifiers. Emuldan contains a mixture of triglycerides, diglycerides, monoglycerides, glycerol and sodium stearate but information acquired could possibly be closely related to real industrial application which is always complex. These different mesophases, if they are formed, are possibly well manifested in their stability and rheological properties. Thus besides determining the stability of the Emuldan/palm olein/water system, one of the objectives of the present study is to determine the rheological changes when the composition of any one of the three components is varied.

5.7 MATERIALS AND METHODS

Neutralised, bleached and deodorised palm olein consisting of C16:0 (38 wt %), C18:0 (4.2 wt %), C18:1 (43.4 wt %) and C18:2 (11.8 wt %) was used. The olein shall also be referred as the "oil" or "palm oil" in this chapter. Emuldan was kindly supplied by Grindsted products A/S and was used as such. The composition is as shown in Tables (1) and (2).

5.7.1 Mapping of Ternary Phase Diagram

Initially the required percentage composition of each component was identified using standard ternary phase diagram. The individual components ie. palm olein, water and Emuldan were weighed into 10 ml test tubes. The total weight of each sample was fixed at 5 gm.

The samples were placed in a water bath maintained at 60°C so as to melt the mixture. The sample was then homogenised for 30 sec. using a DIAX 600 homogeniser with dispersing tool T, after which the samples were placed in a waterbath at 25°C and observed visually. Visual observations of the respective samples were recorded as shown in Fig. 2.

5.7.2 Preparation of Palm Olein-in-Water Emulsion using Emuldan (Samples 1-24)

All sample concentrations were in weight % basis. (wt %). 100g of each emulsion was prepared. The composition of the constituents (wt. %) is as shown in Table 3.

The oil and emulsifier were weighed into a 250ml flask, melted at 60°C overnight and transferred to a waterbath maintained at 60°C. The required amount of water was weighed separately and incubated at 60°C also and then slowly pipetted into the oil within 5 minutes, while stirring at 2000 rpm. The stirrer speed was then increased to 6000 rpm and homogenisation was continued for another 10 minutes. The DIAX 600 homogeniser with 20 G dispersion tool was used.

Foaming occurred during homogenisation. Thus the sample flask was capped and left in a 60°C oven for two hours before being transferred to a 50ml measuring cylinder for creaming test at 25°C. This removed most of the foam.

More viscous samples were poured into small plastic disk of diameter 3.5 cm. while still warm. On cooling to 25°C, the samples solidified. The disk of sample was covered, stored at 25°C and analysed the next day. The

samples were labelled in sequence as shown in the ternary phase diagram (Fig. 3).

5.7.3 Preparation of Emuldan in Water. (Samples A-G)

100g each of Emuldan in water samples was prepared as follows. All sample concentrations were in weight % basis. The required amount of Emuldan (Table 4) was weighed into a flask and kept in a waterbath maintained at 60°C to melt. Water was also heated at 60°C. The required amount of water was slowly pipetted into the Emuldan with stirring under the same conditions as those for samples (1-24) as described above.

5.7.4 Particle Sizing

See Chapter 4, Section 4.2.4 on Materials and Methods.

5.7.5 Rheological Measurements

Rheological measurements were made at room temperature using a HAAKE Rheostress RS100 rheometer, fixed with a water circulator (25°C) at the base of the measuring plate. Various cone-and-plate geometries were used for the measurements.

a) **Flow Curve**. The steady state flow curves of sample 1-12 and A, B were determined by applying an increasing stress and the shear rate was measured. Sample 1-12 A, B and C were measured with a shear stress of 0.01-5 Pa. The cone-and-plate SS 3.5 of 4° angle was used. Computation was carried out using Haake Software VI.3X . The flow curves of samples 13-24 could not be determined because the samples slipped out of the measuring plates at low shear rates.

b) **Creep Test**. The creep and recovery tests were carried out under a constant stress of 5 Pa and 20 Pa for samples 13-18, C and 19-24, D-G respectively. The stress used was within the range of linear visco-elasticity. The samples were tested for 300 seconds for both the creep and recovery. Serrated parallel plate PP 35 of 3.5 cm diameter was used with gap size of 1.5 mm between the two plates.

c) **Dynamic Testing**. Oscillatory experiments were carried out under controlled stress mode using the PP 5 serrated plate of diameter 3.5 mm with a gap of 1.5 mm between the two plates.

An initial stress sweep was done for samples 13-24 to determine the linear viscoelastic region. The frequency used was 1Hz.

The subsequent frequency sweep tests were carried out from 0.1 to 500 rad/s.In data analysis only restricted frequency from 0.1 to 100 rad/s were discussed as in most samples erratic measurements were detected beyond 100 rad/s. Samples 13-18, C and D were determined at a stress of 5 Pa while sample 19-24 and D-G were determined at a stress of 20 Pa.

Dynamic testing was not carried out for samples 1-12 as the lowest stress of the instrument at 0.1 Pa was out of the linear viscoelastic range of the samples.

5.8 RESULTS AND DISCUSSION

5.8.1 Tenary Phase Diagram

The ternary phase diagram of the oil (palm olein) - emulsifier (Emuldan)-water [Fig. 2] indicated several possible mesomorphic phases in equilibrium. Various miscellar, reversed miscellar, isotropic phases have been identified in monoglycerides/oil/water system by X-ray diffraction measurement and polarising microscopy previously (20-24). In this study only visual

observation with respect to obvious phase differentiation was made. The main objective was to determine an approximate concentration range for the three components where a single phase or homogenous mixture is formed. At high concentration of olein of greater than 30 wt % (see Fig. 2 marked Ow) turbid yellowish olein was the major phase with a thin layer of water below. The turbid yellowish layer was probably due to the dispersion of water droplets into the isotropic mixture of Emuldan and olein as Emuldan is soluble in olein but insoluble in water.

At high concentration of Emuldan (greater than 40 wt %) and relatively low concentration of water (less than 30 wt %) and olein (less than 30 wt %) (region marked T), a single turbid phase was observed. At about this region, in the triglycerides (soyabean oil)/monoglyceride (from sunflower oil)/water system, Engstrom (23) identified a miscellar isotropic phase.

The region marked Co is another creamy-like mesomorphic phase together with excess oil which separates into a distinct layer on top on increasing the concentration of olein. Only a drop of oil was observed on the surface of samples marked Co*. On further decreasing the olein concentration, a single cream-like (marked C) phase was observed. At extremely low concentration of olein (<5%)

with at least 40% Emuldan and high concentration of water (marked Ts), a single hard solid phase was observed.

Intermediate between the single phase regions of T and C lies the two phase regions of To and Co. To consists of clear oil and turbid water while Co consists of a white creamy zone with oil on the surface.

In this study, the visually observed single phase, viscous region marked C and Co* were further studied in detail with respect to rheology, sample stability and droplet size.

5.8.2 Creaming Stability

All the samples prepared were opaque white in colour at 60°C. Immediately after preparation, samples 1-18 were pourable and could easily be transferred to a measuring cylinder. Creaming was observed at 25°C. Samples 1-6 (except sample 5) which contained 3 wt % Emuldan with 5 to 30 wt % olein in the emulsion were unstable with respect to creaming (Fig. 4). After a week, phase separation into a concentrated and a dilute layer of cream was observed. The demarcation could only be observed when the samples were observed with an intense light source. It is more of a creaming concentration gradient. No phase separation was observed in samples 7-18, while samples 19-24 hardened immediately

when kept at 25°C. The fluid-like samples 1-12 were all readily redispersable in water. Sample 13-18 were not so easily redispersed in water. No phase separation was observed for sample A-C, even after 3 weeks at 25°C.

5.8.3 Particle Size Distribution

Samples A,B and C containing 3,5 and 10 wt % of Emuldan only in water was found to contain extremely fine droplets ranging from 0.1-1.0 μm with a mean of 0.44, 0.38 and 0.30 μm respectively as shown in Table 5 and Fig. 6. These were probably Emuldan dispersions as all saturated monoglycerides formed dispersions when the water content of the system was higher than that corresponding to a lamellar phase (17). These extremely fine droplets resulted in the extreme creaming stability as mentioned in the creaming test. Sample D-G could not be effectively redispersed in water and thus were not sized.

Emuldan was able to lower the interfacial tension of the palm olein/water interface (Fig. 5). It is thus possible to emulsify olein because oil droplets were formed easily. A bimodal size distribution was noted for some samples (1-4, 7-8 and 13-14) containing Emuldan, water and olein, indicating there were possibly two classes of droplets in the samples (Table 5 and Fig 6-8). The smaller droplets of less than 1 μm were probably those of Emuldan dispersions similar to that of samples

A-C while that of bigger size were that of olein droplets. The droplets with a relatively wide span of 1.75-3.35 also explain the slight phase separation (creaming gradient) observed in the creaming test of samples 1 to 6 except sample 5. The bigger droplets (> 1 μm) creamed to the surface. The extremely narrow droplets size distribution (mean of 0.41, span 1) of sample 5 did not cause any creaming gradient. No creaming gradient was observed in samples 7-18, although droplets of bigger size and wider span were formed. This is probably due to the relatively viscous medium in which the droplets were dispersed.

For overall comparison studies, only the mean particle size will be considered. At low Emuldan in water concentrations of 3.3-16.7 wt % with 5-30 wt % olein in the emulsions (samples 1 - 18), the droplet size ranged from 0.1 to 40 μm with mean diameter of 0.34 to 2.27 μm (Fig. 6-8, Table 5). The span of the size distribution was greatest for samples 1-4 which contained 3.7-4.5 wt % Emuldan in water with 15-30 wt % olein. As the concentration of Emuldan in water was increased in sample 7-18, the mean droplet size was very much reduced.

When the various samples are compared (with reference to Tenary Phase Diagram, Fig. 3) at a fixed concentration of olein, the average droplet size

decreased as the Emuldan in water concentration was increased as illustrated in the samples (1,7,13), (2,8,14), (3,9,15), (4,10,16) and (5,11,17) (Fig. 9). When the concentration of olein in the emulsion was decreased the droplet size also decreased except samples 6,12 and 18 (at the lowest concentration of 5 wt % olein) which did not follow the trend.

At a fixed concentration of Emuldan in the emulsions as illustrated in samples 1-6, 7-12 and 13-18 (Fig. 10) when the ratio of olein to water was decreased, there was a corresponding decrease in the droplet size except at the lowest olein concentration of 5%, relatively bigger droplets were obtained as in sample 6,12 and 18.

There was no clear trend in droplet size distribution when the weight % of Emuldan/Olein was varied (Fig. 11).

5.8.4 Optical Microscopy

Optical micrograph confirms the presence of unaggregated droplets in the samples 1-12 (Fig. 12, 13) but flocs were found in sample 13 (Fig. 14). This contributed to the obvious bimodal nature of droplet size distribution of samples 13 and 14. These flocs were weakly aggregated which could be broken up by greater agitation. Well dispersed smaller droplets were clearly seen in the background of the micrograph. Some free oil

droplets were still present in samples 19-24 as illustrated in samples 20 (Fig 15), however due to difficulty in dilution these droplets could not be sized.

In the ternary system where olein was incorporated, after storing for 3 weeks, crystallisation became evident in some samples, where needle like crystals were observed (Fig. 16). A 6-month-old sample was observed for comparison (Fig. 17). The crystals were relatively bigger and irregular in shape. X-ray diffraction measurement using the Enrafnonius FR590 X-Ray diffractometer confirmed the presence of ß crystals (strong band at 4.6 angstron), probably formed by the monoglycerides Emuldan as olein is a liquid at 25°C. This trend seems to be similar to that of the phenomenon observed as typical syneresis of unstable gel system of monoglycerides (18) indicating that possibly some form of lamellar gel structure could be formed in the present ternary system of Emuldan/oil/water. Further experimental work in determining and comparing the thickness of the bilayer or water layer using low angle X-ray and other complementary methods could possibly elucidate the exact structures formed at certain concentrations of Emuldan, oil and water.

Samples of the binary system containing Emuldan in water showed different structures as observed under the polarising microscope. At low concentration of 3-10 wt %

dynamic oscillatory measurements to determine the viscoelastic properties were carried out on samples 13-24 and C-G. Samples A-G were binary systems that contained various concentrations of Emuldan in water for comparison with the ternary system (samples 1-24) which contained various concentrations of olein, water and Emuldan. The various compositions had been identified using the phase diagram shown in Fig. 3. The constituents of the samples are given in Table 3.

a. Rheological Modelling

Different rheological models have been used to describe the flow properties or viscosities of liquid and semi-liquid food products. The simplest model is one that fits the Newtonian behaviour ie. a linear relationship between the shear stress and shear rate, $\tau = \eta \dot{\gamma}$ where τ (Pa) is shear stress, $\dot{\gamma}$ (s^{-1}) is shear rate and η (Pa s) is the viscosity. η is a constant independent of the shear rate. Many food products, although having an apparent viscosity may exhibit a yield stress, τ_o, where $\tau = \tau_o + K'\dot{\gamma}$ commonly known as the Bingham yield value given by the Bingham Model. Food exhibiting a yield stress is said to show plastic or viscoplastic behaviour. The constant, K', is known as the plastic viscosity.

For non-Newtonian products, the viscosity is dependent on the shear rate. Many models have been proposed for foodstuffs, but generally the simple 2-parameter Ostwald de Waele or Power Law, $\eta_a = K\dot{\gamma}^{n-1}$ suits many products. K is a measure of the consistency factor and n is the flow behaviour index while, the shear rate $\dot{\gamma}$ may cover a limited range of an order of one or two log cycles. This model was found to fit over 200 food products (48). For values of n from 0.1-0.95, the products are known as pseudoplastic and are characterised by a decrease in apparent viscosity, η_a, with increasing shear rate, i.e shear thinning. For values of n=0.95-1.05, the behaviour is essentially Newtonian but ideally n=1. For n values greater than 1.05, the products are referred as dilatant, i.e. shear thickening where the apparent viscosity increases with increasing shear rate.

The three parameters Herschel Bulkley model where $\tau = \tau_o + K\dot{\gamma}^n$ is basically an extension of the Power Law to include a yield stress, τ_o. The existence of a yield stress indicates that there is some form of interactive structures which must be broken down before an appreciable flow can be initiated. In emulsions the attractive van der Waals forces lead to a weak attraction between the droplets, this results in a formation of network structures (38). The yield stress was defined by Blair (49) as the stress below which no flow was observed

under the conditions of the experiment. With the introduction of the constant stress rheometer, shear rate as low as 10^{-5} s^{-1} can be detected, suggesting that the yield stress is merely an artefact of extrapolation. However, Hartnett and Hu (50) had shown, using a falling ball technique, that a yield stress is indeed required to break down the structure before flow can occur.

Some examples of shear thinning food products that fit the Herschel Bulkley model are protein isolates of soya (51), orange juice concentrate (52) and mango puree (53). Versatile computer software has allowed the fitting of the experimental data to various rheological models which may relate to more specific categories of food products. Thus the need for testing of a particular model fit depends on the purpose of the exercise. It could be for quality control, engineering design or the necessity to derive a simple formula to represent a specific system and to correlate other parameters such as concentration, temperature, time or medium of the dispersion to the products. Holdsworth (48) listed as many as 22 models in his review of the rheological models used for the prediction of the flow properties of various food products.

b. Yield Stress

Typical flow curves of the Emuldan/water and Emuldan/oil/water systems are illustrated in Fig. 21, indicating a very low yield stress of less than 1 Pa. The experimental data when fitted to the Herschel Bulkley model generated extremely low Chi square, X^2 values (Table 6). For comparison and uniformity purpose, the yield stress has been limited to the stress corresponding to a shear rate of 0.1 s^{-1} (equivalent to zero shear) as determined using the Haake software VI.3X CS. The yield stress deduced at 0.1 s^{-1} for the Emuldan/water and Emuldan/oil/water systems can provide, in our present modest objective, some basic understanding of the Emuldan/oil/water system. Relatively good fit was obtained from shear rate 0.1 to 100 s^{-1} for samples A,B and 1-12 (Fig. 21).

In the binary systems of 3 wt % and 5 wt % Emuldan in water, the yield stress was only 0.05 and 0.09 Pa respectively. Wayne et.al (54) characterised various commercially processed fluid milk with a rotational steady shear viscometer. By extrapolation of the shear stress versus shear rate plots to zero shear, he obtained very low non-zero intercept which may be considered as the yield stress. Values ranging 0.03-0.07 Pa were obtained which were in same range as that obtained for the Emuldan/water system.

Yield stress of the ternary system of Emuldan/oil/water system is affected by the amount of olein incorporated. Samples 13-24 slipped out of the measurement plate at a relatively low shear rate and could not be measured. On incorporation of 5-30 wt % olein (samples 1-12) which contained 3.3-7.7 wt % Emuldan in water, yield stress from 0.23 to 0.61 Pa were obtained (Table 6). Yield stress of almost the same range of 0.98 and 0.21-7.4 Pa have been obtained for mango pure (53) and strawberry jams (55) respectively.

c. Apparent Viscosity, η_o

Typical viscosity curves of the Emuldan/water system (samples A,B) and Emuldan/oil/water system (samples 1-12) are illustrated in Fig. 22. The viscosity curves show that all the samples exhibited shear thinning behaviour with the viscosity reaching a limiting value at higher shear rate. Good fit with the Herschel Bulkley model was obtained (Table 6) with excellent correlation (low χ^2 values). Using the Herschel Bulkley model, the K values obtained for the various Emuldan/oil/water samples were low (Table 6). All n values were less than 1, indicating the samples were pseudoplastic in nature.

Samples were compared using the Herschel Bulkley model fitted within the shear rate range of $0.1\text{-}100s^{-1}$. Fig. 22 showed that for Samples A, B, the experimental and the derived Herschel Bulkley model fit relatively well up to shear rate $200s^{-1}$. For samples 1-12 they fit well up to a lower shear rate of $50s^{-1}$ and at higher shear rates deviation from Herschel Bulkley model occurred.

A plot of η_{30} against the weight % of Emuldan in water (Fig. 23) showed that for the binary system (samples A,B) there was an increase in apparent viscosity from 2.81 to 28.9 mPa s as the concentration of Emuldan/water was increased from 3 to 5 wt %. When 15-30 wt % oil was emulsified at 3.7-4.5 wt % Emuldan in water (samples 1-4), η_{30} of the emulsions increased correspondingly to peak at 26.8 mPa s. However with incorporation of only 5-10 wt % olein with 3.3-3.4 wt % Emuldan in water (samples 5,6) η_{30} is relatively higher than the apparent viscosity of the binary system at the same relative concentration of Emuldan in water. Various commercially processed fluid milk measured have apparent viscosity ranging from 1.6-2.3 mPa.s at $121\text{-}486s^{-1}$ (54).

Samples 7-10 containing 6.3-7.7 wt % Emuldan in water with 15-30 wt % olein incorporated seem to possess a linear relationship of η_{30} with the concentration of Emuldan in water, similar to that for samples 1-4.

However, at 5.9 and 5.6 wt % Emuldan in water and when the olein concentration was decreased to 5 and 10 wt % respectively (samples 11,12), η_{30} is increased again similar to that observed for samples 5 and 6. Although samples 8-12 have a higher concentration of Emuldan (5.6-7.1 wt %) in water η_{30} was not significantly higher than those for the binary system that contains 5 wt % Emuldan in water. Samples10-12 have lower η_{30} compared to sample B.

There seems to be two categories of Emuldan/oil/water system. Based on the apparent viscosity, η_{30} behaviour, one category containing less than 5.0 wt % Emuldan in water where incorporation of olein either has negligible effect on η_{30} or only slight increase η_{30}. For another group containing 5.0-7.0 wt % Emuldan in water the viscosities were reduced in the presence of olein when compared to the binary system of sample B which contained 5.0 wt % Emuldan in water. Sample 7, which contained 30 wt % olein with 7.7 wt % Emuldan in water, had a very high η_{30} of 71.1 mPas and did not fall into either of the two categories.

The incorporation of olein into Emuldan/water system resulted in the formation of oil droplets which were much larger than the particles found in the binary system. These gave rise to different interactive forces resulting in different flow properties. Emulsions with

smaller size droplets tend to be more viscous compared to coarser system (38). The flow properties of the ternary system was further affected by changes in phase volume consisting of two different dispersed materials: oil and Emuldan. Different oil concentrations or phase volumes can change not only the viscosity but subsequently become viscoelastic at very high phase volume as in the soyabean oil-in-water emulsions (56).

5.8.5.2 Viscoelastic Properties

The physical characteristics of various food systems can be characterised by combining the elastic and viscous behaviour. This behaviour of material displaying both solid and liquid-like properties is generally termed the viscoelastic properties. The viscoelastic properties of many food systems may be studied using various rheological instrumentations and methods (57). Samples C-G containing 10-30 wt % Emuldan in water and samples 13-24 which contained 11.8-27.3 wt % Emuldan in water with 5-30 wt % olein incoporated were determined to be viscoelastic. Two methods shall be used in characterising the Emuldan/water and Emuldan/oil/water systems: that is the Creep Recovery Curves and Oscillatory Testing under controlled stress. These analysis were all carried out in the linear viscoelastic region using the HAAKE Rheostress RS100 rheometer.

a. Creep Recovery Measurements

Some food systems that have been studied using the Creep Recovery tests are eg. dough and bread (58), oil-in-water emulsions (59), mayonnaise (60), salad dressings (61), meat emulsions with fat as the dispersed phase and proteinaceous medium (62), hydrocolloids (63) and solid foods such as cheese, sausages, potatoes and peas (64), butter, margarine (65) and ice creams (66). Besides food, studies on the viscoelastic properties of some paracrystalline phases of the surfactant, polyoxyethylene (POE) derivatives of oleic alcohol/water/mineral oil systems have also been studied by the creep recovery measurement (47).

In a creep-recovery experiment, a constant stress is applied instantaneously at time t=o and the stress response (known as Creep) is monitored (Fig. 24) over time t sec. The stress is then released instantaneously and the response (known as Recovery) monitored for another t sec. The two responses are illustrated in the Creep-Recovery curve (Fig. 24) where compliance (ratio of strain/stress, Pa^{-1} is plotted against time.

The creep recovery curve has several distinct regions (Fig. 24). On application of the instantaneous stress there is an instantaneous elastic compliance J_o, represented by AB. The compliance rises slowly to C

beyond which the compliance increases linearly with time. The region BC represents the retarded elastic compliance, J_e, while CD represents the Newtonian compliance. When the stress is removed at D, the compliance recovers instantaneously (DE) followed by elastic recovery (EF) and an eventual flattening of the curve. The vertical height at time 2t illustrates the non recoverable compliance which is related to the degree of structural alteration incurred by the sample during the test. The steady state compliance, J_eo, which is the sum of J_o and J_e represents the elastic component of the system while the zero shear viscosity, η_o, which may be deduced from the gradient of the Newtonian compliance, J_n represents the viscous component.

Fig. 25 and 26 illustrates the typical Creep Recovery curves of the binary system of Emuldan/water and the ternary system of Emuldan/oil/water respectively. All the samples are viscoelastic liquids as evidenced by the final non-zero compliance indicating the occurrence of irreversible flow on the creep side. Food emulsions such as mayonnaise (60), soyabean oil/water emulsions of various phase volume (59) and the hexagonal mesophase of the ether linked non ionic surfactant (polyoxyethylene derivative of oleic alcohol) (47) were found to behave as viscoelastic liquids too. The creep-recovery behaviour of various food systems may be modelled with various mechanical models consisting of a combination of

the basic spring and dashpot representing the viscous and elastic component respectively. Kiosseoglou and Sherman (60) interpreted the various oil in water emulsions and mayonnaise results by mean of a six-parameter model while Parades et al. (61) in his studies on salad dressings used a four-parameter model to fit the system. Orecchioni et al. (47) attempted modelling of the creep recovery curve of the hexagonal phase of POE of oleic alcohol using a six-parameter model.

As a preliminary attempt to characterise the viscoelastic properties of the Emuldan/oil/water system, the elastic component is discussed with respect to the steady state compliance, J_eo and the viscous component as represented by the zero shear viscosity, η_o The results are shown in Table 7.

The steady state compliance, J_eo of the Emuldan/water system (sample C-G) decreased linearly from 4.89×10^{-3} to 4.20×10^{-5} Pa^{-1} as the concentration of Emuldan in water was increased from 10 to 30% (Fig. 27). The lower compliance indicated that the samples became less liquid and thus less flexible and perhaps even brittle. The zero shear viscosity increased from 7.30×10^{3} to 8.22×10^{6} Pa.s as the concentration of Emuldan in water was increased from 10 to 30 wt % in water (Fig. 28). Orecchioni (47) found in hexagonal

mesophase of the surfactant POE ether-linked water system a retarded elastic compliance in the range of 10^{-6} Pa^{-1} and instantaneous compliance, J_o of 10^{-6} Pa^{-1} with a zero shear viscosity, η_o in the range of 10^7 Pa.s. Extremely low or no retarded elasticity was detected in the lamellar phase but an instantaneous elasticity of $1x10^{-5}$ Pa^{-1} was reported. These values seem to be an order of magnitude lower than that observed for the Emuldan/water system at the concentration range (10-30 wt %) studied but it is not surprising as no obvious liquid crystals of hexagonal phase were observed except sample D where lamellar phases were observed. Even than, sample D has an instantaneous compliance in the range of 10^{-3} Pa^{-1} which is greater than the lamellar phase of POE ether-linked/water system of 10^{-6} Pa^{-1} (47).

The ternary system of Emuldan/oil/water (samples 13-24) containing 11.8-27.3 wt % of Emuldan in water with various concentration of olein (5-30 wt %) gave $J_{e}o$ values ranging from 1.441 x 10^{-1} to 7.754 x 10^{-4} Pa^{-1} while the η_o varied from 7.544 x 10^2 to $4.478x10^6$ Pa.s (Table 7). Both the $J_{e}o$ and η_o came within the range of those of the binary system having the same concentration range of Emuldan. In the soyabean oil emulsion system with 1% Xanthan and at phase volume of 0.2 to 0.7, a retarded compliance in the range of 10^{-2} Pa^{-1} and η_o of 1 x 10^4 - 1 x 10^5 Pa s were observed (59).

Fig. 27 shows the steady state compliance of samples C-G and 13-24 respectively with olein incorporated plotted against the concentration of Emuldan in water. The steady state compliance, J_e^o decreased linearly as the concentration of Emuldan in water was increased for samples C-G. Sample E containing 20 wt % Emuldan had a lower compliance than sample F containing 25 wt % Emuldan in water. This indicated that sample E was probably more structured than sample F, as a result of the formation of some structures (Fig. 20) which were less compliant than those of the lamellar formed with 15 wt % Emuldan in water (sample D, Fig.19). Further increase of Emuldan to 30 wt % in water reduced the compliance.

The steady state compliance, J_e^o decreased as the concentration of Emuldan in water was increased in the samples containing various concentrations of olein (5-30 wt %) given by samples 13-24. Compared to the binary system (sample C-G), olein incorporation increased the compliance of the emulsion by a factor of 10 except samples 17 and 18. These two samples contained the least concentration of Emuldan in water at 12.5 and 11.8 wt % respectively. In view of their relatively fluid nature they did not follow the trend in compliance.

In the binary system of Emuldan/water, the zero shear viscosity, η_o increased as the concentration of

Emuldan in water was increased (Fig. 28). With incorporation of olein (samples 13-24), the zero shear viscosity was slightly decreased. Again samples 17 and 18 which were fluid-like had the lowest η_o compared to this group of samples.

Thus it is concluded that the incorporation of 5-30 wt % olein in system containing 13.3-27.3 wt % Emuldan did not affect the viscoelasticity of the system significantly as reflected in the creep recovery measurements.

b. Dynamic Oscillatory Measurements

Besides using the Creep Recovery method, the rheological behaviour of viscoelastic systems may also be studied using the dynamic oscillatory technique. The procedure consists of imparting a sinusoidally varying stress or movement of known frequency, ω, to the sample (Fig. 29). The stress causes a strain to arise in the sample, which is oscillating at the same frequency but may be out of phase with it by an angle δ. The phase shift is dependent on the viscoelastic nature of the material. In a liquid the stress strain will be completely out of phase while in a solid there will be no phase shift. A material which is both viscous or elastic will have a shift between 0-90°.

The relationship between the stress (σ) and strain ($\dot{\gamma}$) is defined as $\sigma_o = G^*(\omega)\dot{\gamma}_o$ where G* is the complex modulus from which complete information on the properties of the material can be obtained. For the stress rheometer, the stress σ_o and frequency ω are set while the strain $\dot{\gamma}_o$ is measured. Using classical mathematics the complex modulus is represented as G*=G'+ iG" where G' is the elastic/storage modulus and G" is the viscous/loss modulus where i= $\sqrt{-1}$. With the advancement in microcomputer all the data analysis can be undertaken in accordance with the equations using the Haake V1.3 software.

Oscillatory measurements can be carried out over a wide range of frequencies. However, if fundamental parameters are required, it is necessary to restrict it to the linear viscoelastic region where G* and thus G' and G" are independent of the stress. In this region the structure of the matrix is not destroyed during shear. Therefore the moduli are only a function of the frequency, ω. From the measurement of the strain and stress amplitude and the associated phase lag δ, the viscoelasticity property can be deduced.

The limit of viscoelastic linearity can be detected by running a stress sweep of the samples at a fixed frequency (67). Beyond the linear range, the internal

structures, network formation due to molecular bonds or aggregates are destroyed. Shear thinning takes place and a major part of the introduced energy will thus be lost as heat, giving rise to an erratic modulus change. Thus the linear viscoelastic range is limited to the stress for which G* is a constant. Useful data regarding the viscous moduli G' and elastic moduli G" may then be used to characterise the system.

Oscillatory measurements have been used in the understanding and development of new food products with respect to its viscoelastic properties such as those of dough (68), cheese (69) and Surimi sea food products (70). Different types of protein at different pH, electrolyte concentrations and temperature have been shown to exhibit different viscoelastic rheological properties (71, 72). Various hydrocolloids, used either singly or in combinations at different concentrations may also exhibit various viscoelastic properties (73-75). Similarly such technique has been used in the study of liquid crystalline structures of surfactants in water (46,47,76-77) and the effect of salt and hydrocarbon incorporation into the liquid crystalline structures (78). Viscoelasticity is also studied in various nonfood types of concentrated dispersions (79-81), using the oscillatory technique. In real food systems, the matrix can be influenced by fillers such as air bubbles, crystalline ice or fat,starch granules and proteins (82-84). As a result

of the modification of the matrix, the elasticity and viscosity of the system will vary resulting in measureable amounts of G' and G" which are determinable using oscillatory measurements too.

b(i). Stress Sweep Measurements

The molecular orientation of the polar lipids in their lamellar crystalline phase (Fig. 1) is such that the lipids are oriented in bilayers with the polar groups "head to head", separated by layers of solid hydrocarbon chains usually packed in a double chain-length mode. In liquid crystals the hydrocarbon chains are "melted" but may still adopt a sort of disordered liquid-like state held closely packed together by the weak van der Waals interactive forces. When polar insoluble lipid crystals are mixed with water they swell and form lyotropic liquid crystals depending on temperature and concentration. The driving force (so called hydration forces) behind the formation of lipid water phase is the tendency to hydrate the polar head group while the hydrocarbon chains are kept together in bilayer regions, separated from the water (15). The polar groups are held together by strong ionic and hydrogen bonds, and electrostatic forces interact in between the bilayers of the intervening water layers. The gel phase is a special structure related to the lamellar liquid crystalline phase where it also consists of water layers alternating with lipid bilayers,

but the hydrocarbon are crystalline (Fig. 1). Ionic lipids may swell to a very high water content in the presence of ions giving rise to a thick water layer (14).

Typical stress sweep (Fig. 30) of the Emuldan/water system shows linearity in the various moduli at certain shear stress range. At each particular concentration of Emuldan in water, there is a critical stress beyond which the respective moduli will be altered due to a breakdown of the structures. This maximum stress denotes the limit of the linear region and is termed the Critical Stress, τ_c.

Sample C containing 10 wt % Emuldan in water has the lowest critical stress of 3.4 Pa (Table 8). τ_c reaches a maximum of greater than 500 Pa at 30 wt % Emuldan in water. Optical microphotograph shows obvious textures corresponding to those of lamellar crystal structure in sample D which contains 15 wt % Emuldan in water. The critical stress for the destruction of lamellar mesophases of the 15 wt % Emuldan in water system is at 61.1 Pa. As the concentration of Emuldan in water is increased from 20 to 30 wt % (samples E-G) there will a corresponding increase in the lamellar microdomain. Secondly, the interactive forces among the lamellar microdomain could also be increased accordingly thus

requiring higher critical stress in the range of 200-500 Pa to overcome the structures.

The various moduli G*, G', G" and tan δ at the critical stress are also shown in Table 8. The elastic component G' constituted the major component of G*. The storage moduli were always about an order of magnitude higher than G" (Fig. 31). Sample E containing 20 wt % Emuldan in water has a G' of 98,700 Pa. Further increase of Emuldan in water concentration to 30 wt % resulted in negligible increase of G' to 106,000 Pa. A low value of less than 0.3 was obtained for tan δ which also indicated that the ratio of elasticity to viscosity was high for the Emuldan in water system.

Ternary system containing Emuldan/oil/water ie. samples 13-18 containing 11.8-16.7 wt % Emuldan in water with 5-30 wt % olein have critical stresses that ranged from 1.8 to 43.3 Pa (Table 8, Fig. 32). This τ_c range is comparable to that of samples C and D of the binary system, (τ_c was 3.4-61.1 Pa) which contained 10 and 15% Emuldan in water respectively. The various moduli at the linear range is shown in Table 8. Similar to the binary system of Emuldan/water, the elastic component, G' dominated G* and G" was generally less than G' (Fig. 33). tan δ was all less than 0.30 except sample 18. At the linear viscoelastic region, sample 18 shows a G" value of 17.6 Pa which was greater than G' of 8.84 Pa,

resulting in a tan δ of 2.0. Sample 18 contained 11.8 wt % Emuldan in water with 5 wt % olein and the viscous component, G", predominated over the elastic component G'. The sample was more viscous than elastic. Sample 18 was visually observed to be more fluid than the rest of the samples. The critical concentration of Emuldan/water seemed to be at 12.5 wt % (sample 17) and at this concentration as much as 10 wt % olein could be incorporated and the emulsion could still retain its elastic dominating property.

At the higher range of 18.7-27.3 wt % Emuldan in water and with the incorporation of 5-30 wt % olein (samples 19-24), τ_c ranged from 72 to 300 Pa (Table 8 Fig. 34). This τ_c range is comparable to that of the binary system of 20-30 wt % Emuldan in water (200-500 Pa). The elastic moduli G' predominates over the viscous moduli, G" (Fig. 33).

Compared to the binary system, samples C-G at the same concentration of Emuldan in water, the critical stress of the ternary system, samples 13-24, was generally slightly reduced (Fig. 35), indicating that the lamellar structures of those in the binary system may still be present in the ternary system.

Creep measurements have been used to study some paracrystalline phases appearing in the ether linked polyoxyethylene derivatives of oleic alcohol/mineral

oil/water system where as much as 18-33 wt % mineral oil could be incorporated without any change to the crystalline structure while rheological changes were noted when the concentration of surfactant was varied (47). Vasquez (78) reported a decrease in G' and G" in the linear viscoelastic region when 1-4 wt % decane was added to the Aerosol OT/brine water system. He postulated that decane swells the bilayers and locates itself in the centre of the hydrocarbon layer, far away from the polar head palisade which then provide a more fluid hydrocarbon layer. This facilitates the movement of bilayers and microdomain under shear. Jiang (85) studied the phase behaviour of the polyoxyethylene 10 steryl ether/geraniol/olive oil/water/oil system using X-ray to determine the interlayer spacing of the bilipid and water layers. He postulated that olive oil was partitioned between the terminal methyl group of the hydrocarbon chains of the surfactant. When these are saturated the oil became localised in the hydrocarbon chains, the lamellar liquid structures would be destabilised. The Emuldan/ water system could possibly be comparable to the polyoxyethylene 10 steryl ether/ geraniol/olive/water system as the monoglyceride Emuldan has one ester chain with a terminal methyl group which will be favorable for triglyceride "solublisation", in addition to having the triglycerides located in between the hydrocarbon chains. These molecular interactions of

the oil and hydrocarbon bilayers together with hydration and ionic forces at the water layer play an important role in the viscoelastic behaviour of the Emuldan/water/olein system. The Emuldan used was analysed to contain 13.0 wt % glycerol which is possibly favourably associated with the aqueous layer modifying the electrostatic, polar and ionic force involved and thus affecting the water layer thickness. Incorporation of olein contributes to structural modification because under the microscope no obvious lamellar structures were observed. This, however cannot exclude the possibility of formation of other isotropic structure which could not be visible under the microscope. Excess olein in emulsified droplets also contributes to variable viscoelastic behaviour of the Emuldan/water/olein system.

In the range of 12.7-16.7 wt % Emuldan in water and with the incorporation of 10-30 wt % olein (samples 13-17), a linear increase in elastic moduli G' with increased concentration of Emuldan in water (Fig. 36) similar to that of the binary system of 10-15 wt % Emuldan in water (samples C,D,E) was noted. However, sample 18 which contained 11.8 wt % Emuldan in water with 5 wt % olein has the lowest G' value.

At a higher concentration of 18.7-27.3 wt % Emuldan in water with 5-30 wt % olein (samples 19-24) the storage moduli, G' were lower compared to the binary

system at the same concentration of Emuldan in water. Samples 20, 21 and 23 which contained 25.0, 23.1 and 20.0 wt % Emuldan in water with 25, 20 and 19 wt % olein respectively seemed to indicate a linear correlation of G' with the % weight concentration of Emuldan in water. However, in the binary system of 20-30 wt % Emuldan in water (samples E-G) the storage moduli G' seemed to have reached a maximum and constant value in the linear viscoelastic region.

b(ii). Frequency Sweep Measurements

The mechanical spectra (modulus vs frequency plot) of the Emuldan/water system (sample C-G) is shown in Fig. 37. The elastic modulus G' completely dominated the complex modulus G* at the frequency range ω, 0.05-100 rad/s. Thus the viscous moduli, G" was relatively insignificant compared to G'. The general trend of the spectra show some similarity to that of hydrocolloid gels such as aqueous guar galactomannan at 3 wt % water (73), 1.4 wt % alginate gel (74) and 0.5-1 wt % k-carrageenans (75) although the absolute moduli vary.

Some commercial mayonnaise at specific temperature (86) and the Aerosol OT/water system at 20-70 wt % concentrations (47) also had similar mechanical spectra but again their absolute G' and G" values were different. Generally, in these systems, the shear moduli G' and G"

show very weak dependency on the frequency, ω. G' was dominant and increased slightly with frequency while G" was smaller and relatively insensitive to frequency change.

For the Emuldan/ water system, there seemed to be a cross over of G' and G" values at extremely low frequency (Fig. 37). This indicated that at very low frequency ie. long relaxation time, the system was able to dissipate the energy but at higher frequency the energy was all stored.

In the binary system of Emuldan/water, the elastic moduli,G' were strongly dependent on the concentration of Emuldan in water over the frequency range of 0.05-100 rad/s as illustrated in Fig.37. G' increased from 20 to 80 Pa for 10 wt % Emuldan in water (sample C); from $4x10^3$ to $8x10^3$ Pa for 15 wt % Emuldan in water (sample D) and $1x10^4$ to $1x10^5$ Pa for samples containing 20 wt % Emuldan in water (sample E). Samples F and G which contained 25 and 30 wt % Emuldan in water respectively have nearly identical moduli as sample E. Relatively low G" of approximately 20, 200 and 20,000 Pa respectively were found for samples containing 10,15 and 20-30 wt % Emuldan in water.

Fig.38 illustrates the mechanical spectra of the ternary system of samples 13-18 which consists of Emuldan, oil and water. Generally the elastic component,

G' dominated over the viscous moduli, G", in the frequency range of 0.05-100 rad/s, except for samples 17 and 18 which contained low concentration of Emuldan in water in this group of samples. In sample 17 (12.5 wt % Emuldan in water with 10 wt % olein) there was a cross over of G" dominance to G' dominance at frequency above 0.3 rad/s. This possibly indicates some form of ionic bonding modification of the samples at the critical frequency, switching from being viscous to more elastic form. Cross over of moduli in the locust bean gum and kappa-carrageenan mixture system of hydrocolloids was attributed to the sol-gel transition related to the mechanism of gelation of the structurally different hydrocolloid molecules (87). Crossover at the critical frequency in the cetyltrimethylammonium/water system (77) has been attributed to the elongation of miscellar structures. Sample 18 which contains 11.8 wt % Emuldan in water with 5 wt % olein has a viscous modulus, G" that predominates over the elastic, modulus G'at the frequency range from 0.05-100 rad/s. This is supported by visual observation of the samples which was found to be liquid-like and pourable.

At higher concentration of Emuldan in water with various concentration of olein incorporated as illustrated in Fig. 38 with samples 13 (16.7 wt % Emuldan in water with 30 wt % olein) and sample 15 (14.3 wt % Emuldan in water with 20 wt % olein), the mechanical

spectra showed trend similar to that of the binary system of samples D-G which contained 15-30 wt % Emuldan in water. However, the absolute G' and G" values differed significantly. The ternary system having nearly similar concentration of Emuldan in water but with olein incorporated showed much lower moduli compared to the binary system (see Fig. 37,38).

Samples containing 18.7-27.3 wt % Emuldan in water with 5-30 wt % olein incorporated (samples 19-24) (Fig. 39) have comparable mechanical spectra as those of the binary system containing 20-30 wt % Emuldan in water (Binary systems of 20-30 wt % Emuldan in water have insignificant differences in the mechanical spectra). The moduli of the ternary system with about the same concentration of Emuldan in water but with olein incorporated were lower than those of the binary system. Incorporation of olein lowered G* and thus G' and G", but G'was still predominating. However the reduction in the respective moduli became less significant as the concentration of Emuldan in water is increased to 25 and 27. wt % respectively even with 25 and 30 wt % of olein incorporated (samples 19, 20); they have nearly identical moduli as the binary system containing 25-30 wt % in water (see Fig. 37,39).

5.9 CONCLUSION

In view of its viscous and viscoelastic properties, impure mixtures of monoglycerides such as Emuldan may possibly be used as a thickener similar to gelatin, hydrocolloids of alginate, xanthan, carrageenan, guar gum and pectin (41). Rheological measurements indicate that Emuldan/water/oil systems have similar functional properties of some of these food gels. 5-30 wt % olein can be incorporated without changing significantly its rheological characteristics. Hancock (44) proposed that xanthan gum contributed to the emulsion stability of oil-in-water emulsions by two mechanisms. Firstly, part of the xanthan gum is adsorbed at the oil/water interface, thus lowering the interfacial tension and favouring droplet formation. Secondly, the remaining xanthan gum forms liquid crystals in the viscous water phase and stablises the emulsion by physically trapping the emulsion droplets in the microgel matrix. This seems to bear some similarity to the function of Emuldan in oil droplet stablisation in samples 1-12 that contain triglycerides droplets which are stabilised by the polar lipid Emuldan.

Similarly, Friberg (14) has proposed that lamellar multilayer can stabilise emulsion droplets. During emulsification, vigorous stirring of the system could

lead to bimolecular leaflets of lamellar liquid crystals being scattered throughout the continuous phase. These leaflets may form bridges between the dispersed droplets, increasing the macrorigidity of the system. In addition, the multilayer structure may reduce the van der Waals attractive forces thereby inhibiting coalescence.

Samples of the binary system containing Emuldan in water showed different optical textures under the polarising microscope. At low concentration of 3-10 wt % Emuldan in water (samples A-C) optical pattern of lamellar liquid crystalline structure characterised by appearance of Maltese crosses were observed (Fig. 18). At a higher concentration of 15 wt % Emuldan (sample D) another birefringent optical texture of a straited type of lamellar liquid crystalline structure was observed (Fig.19). At higher concentration of 20 wt % Emuldan the optical structures became not so clear cut (Fig.20). It was noted that no such obvious optical pattern was observed in the tenary system of samples 1-24 which contained Emuldan,water and olein.

In the more fluid-like samples 1-12 viscosity changes were attributed to the different types of particles formed by both the oil and Emuldan, and the incorporation of olein into the Emuldan dispersions.

In the more viscous and solid-like samples the various viscoelastic rheological properties of the binary

system of Emuldan/water (samples C-G) are due to the formation of liquid crystal structures. The ternary system of Emuldan/water/oil (samples 13-24) may possibly retain some of the structures as the viscoelastic properties do not differ significantly especially samples containing more than 25 wt % Emuldan in water. In protein gel system, the gel strength and elastic moduli variations are attributed to the number of cross links in the network of the macromolecules and the molecular weight of the proteins (63) while that of hydrocolloid gelation being due to formation of specific junction zones (40) forming a network. The viscoelastic properties of the Emuldan/water/oil is due to interactive forces of the polar and hydrocarbon chains leading to self assembly of surfactant, water and oil giving rise to specific orientated crystalline structures of the molecules together with the oil droplets. Rheological measurements together with other complementary instrumentations like X-Ray diffraction, differential scanning calorimetry, H-NMR and microscopy (76,77,85,88) could provide a better understanding of the structural and interactive forces involved in the formation of liquid crystal structures with olein incorporation.

In this study, the compositions of the ternary systems samples were based on visually homogeneous sample formation. A better basic understanding of the system could be derived by a more thorough, systematic control

of the respective constituents in minor progressions to give a more extensive mapping of the ternary diagram, such that the boundary of the various phases can be clearly defined using various complementary techniques. The critical concentration and role of the sodium stearate and glycerol in affecting the swelling of the monoglycerides mixture used; the maximum amount of olein which could possibly be incorporated into the Emuldan/water system and the significance of the oil droplets in the Emuldan/water system at high and low Emuldan concentrations with respect to other physical properties related to palm oil utilisation both in food and non-food system should be further studied. Such fundamental data would be extremely useful to the Malaysian palm oil industry for more diverse products formulation.

REFERENCES

1. I. Hitoshi, K. Yasushi, S. Kesatoshi (Assignee to Kao Corp., 1992). Manufacture of Bread with Saturated Monoglycerides and Unsaturated Diglycerides. *Jap. Pat. 90331756.*

2. T. Shinji , O. Yasuo (Assignee to Asahi Denka Kogyo K.K., 1991). Oil-in-water Emulsified Fat and Oil Compositions for Bakery Products. *Jap. Pat. 9033499.*

3. H. Toyoji, M. Yutaka (Assignee Snow Brand Milk Products Co. Ltd.,1988). Oil-in-water Emulsions for Whipped Creams. *Jap. Pat. 88267250 A2.*

4. W.Hubertus (1992). Frankfurter-type Sausage Mixtures. The Stability and Distribution of Emulsifiers. *Fleischwirt schaft*, **72**, 53-57.

5. Functional Ingredients for Foods. Grindsted Products, Edwin Rabrs Cej. 38, DK 8220 Brabrand, Denmark.

6. M.C. Chow. Unpublished Data, Palm Oil Research Inst. Malaysia.

7. Y.M. Choo , S.C. Yap (1991) Synthesis of Mono-and-Diglycerides from Palm Oil and Palm Oil Products. *Proceedings PORIM International Palm Oil Conference*, Kuala Lumpur, Malaysia, 132-137.

8. D. Last (1991). Functional Food Ingredient for Palm Oil. *Proceedings PORIM International Palm Oil Conference*, Kuala Lumpur, Malaysia, 127-131.

9. R. Jeppsson (1972). Effects of Barituric Acids using an Emulsion Form Intravenously. *Acta Pharm Suecica*, **9**, 81-90.

10. D.P. Moran (1993). Reduced Calorie Spreads. *PORIM Technology*, **15**, Palm Oil Research Inst. Malaysia.

11. C.Gallengos,M.Berjano,L.Choplin (1992). Linear Viscoelastic Behaviour of Commercial and Model Mayonnaise. *J. Rheology*, **36**(3), 465-478.

12. Malaysian Standard. MS 779 (1982). Specification for Margarine.

13. E.S. Lutton (1965). Phase Behaviour of Aqueous Systems of Monoglycerides. *J. Ame. Oil Chem. Soc.*, **42**, 1068-1070.

14. N.J. Krog (1990). Food Emulsifiers and their Chemical and Physical Properties. *Food Emulsions*, K. Larsson and S. Friberg, Edi. Marcel Dekker, New York, 127-180.

15. N. Krog , A. P. Borup (1973). Swelling behaviour of Lamellar Phases of Saturated Monoglycerides in Aqueous System. *J. Sci. Food and Agric.*, **24**, 691.

16. K. Larsson and N. Krog (1973). Structural Properties of the Lipid Water Gel Phase. *Chem. Phys. Lipids*, **10**, 177.

17. K. Larsson (1967). The Structure of Mesomorphic Phases and Micelles in Aqueous Glyceride Systems, *Zeit. Phys. Chem. Neue Folge*, **65**, 173.

18. N. Krog, J.B. Lauridsen (1976). Food Emulsifiers and their Associations with Water. *Food Emulsions* , S.Friberg, Edi., Marcel Dekker, New York, 67-139.

19. N. Krog, K, Larsson (1968). Phase Behaviour and Rheological Properties of Aqueous System of Industrial Distilled Monoglycerides. *Chem. Phys. Lipids* **2**, 129.

20. W. Hemker (1981), Associative Structures of Polyglycerol Esters in Food Emulsions. *J. Ame. Oil Chem. Soc.* **81**, 114-119.

21. Rydhag (1982). Dispersion of Lamellar Liquid Crystals in Water and Water-Oil Systems, Ph.D. Thesis, University of Lund, Sweden.

22. M. Lindstrom, H. Ljusberg-Wahren, K. Larsson and B. Borgstrom (1981). Aqueous Lipid Phases of Revelance to Intestinal Fat Digestion and Absorption. *Lipids*, **16**, 749.

23. L. Engstrom (1990). Aggregation and Structural Changes in the L2-phase in the System Water/Soybean oil/Sunflower oil Monoglycerides. *J. Dispersion Science Tech.*, **11**(5), 479-489.

24. T.Gulik and K. Larsson (1984). An Electron Microscopy Study of the L2-Phase (Microemulsion) in a Ternary System: Triglyceride/Monoglyceride/Water. *Chem. Phys. Lipids*, **35**, 127-132.

25. S. Friberg and L. Mandell (1970) Phase Equilibriam and their Influence on the Properties of Emulsions. *J. Ame. Oil Chem. Soc.*, May, 149-152.

26. F. Lachampt, R.M. Villa (1966). A Contribution to the Study of Emulsions. *Ame. Perfumer and Cosmetics*, **82**, 29-36.

27. F. Colelles., V. Megias., J. Sanchez., J.L. Parra, J. Coll., F. Balageur, C. Pelejero (1989). Applications of Ternary Systems in Specific Cosmetic Formulations. *Int J. Cosmetic. Sci.*, **11**, 5-19.

28. S. Hamdan ,C.R. Laili (1993). RBD Palm Olein in a Lamellar Liquid Crystalline Structure of Mixed Surfactants I. Optical Pattern and DSC Investigation *Elaeis* **6**, 65-68.

29. S. Friberg L. Mandell and M. Larsson (1969). Mesomorphous Phases - A Factor of Importance for the Properties of Emulsions. *J. Coll. Interface Sci.*, **29**, 155-166.

30. N. Pipel, M.E. Rabhani (1987). Formation of Liquid Crystals in Sunflower Oil in Water Emulsions. *J. Coll. Interface Sci.*, **119**, 550-558.

31. M. Kako and S. Kondo (1978). The Stability of Soybean Oil-Water Emulsions containing Mono and Diglycerides. *J. Coll. Interface* Sci., **69**, 163-169.

32. G. Doxastakis and P. Sherman (1984). The Interaction of Sodium Casseinate with Monoglyceride and Diglyceride at the Oil-water Interface in Corn oil-in-water Emulsions and its Effect on Emulsion Stability. *Colloid Polymer Sci.*, **262**, 902-905.

33. M.J. Reewe & P. Sherman (1988). The Interaction of Modified 7S Soy protein with Mono-and Di-glycerides at the Oil-water Interface and its Effect on the Stability of Concentrated Corn oil-in-water Emulsions. *Colloid Polym. Sci.*, **266**, 930-936.

34. A.M. Vesala and J.R. Rosenholm (1985). Increasing the Stability of Vegetable Oils Solutions with the Aid of Monoglycerides and Cosurfactant *J. Ame. Oil Chemist Soc.*,**62**, 1379-1385.

35. Th. F. Tadros (1992). Rheological Properties of Emulsion Systems. *Emulsions: A Fundamental and Practical Approach.*, J.Sjoblom, Edi., Kluwer Academic Pub., Netherlands,173-188

36. Y. Otsubo & Prud'homme (1994). Rheology of oil-in-Water emulsions. *Rheologica Acta*, **33**, 29-37.

37. Y. Otsubo and R.K. Prod'homme (1994). Effect of Drop Size Distribution on the Flow Behaviour of Oil-in-water Emulsions. *Rheologica Acta*, **33**, 303-306.

38. R.R. Rahalkar (1992). Viscoelastic Properties of Oil-Water Emulsions. *Viscoelastic Properties of Foods*. J.F. Steffe, M.A. Rao, Edi., Elsevier, England, 317-354.

39. K. Suzuki, T. Maeda, K. Matsuoka, K. Kubota (1991). Effect of Constituent Concentration on Rheological Properties of Corn Oil-in-Water Emulsions. *J. Food Science*, **56**, 796-798.

40. D. Oakenfull (1978). Gelling Agents. *CRC Critical Review in Food Science and Nutrition*, **26**, 25-50.

41. N. Garti and D. Reichman (1993). Hydrocolloids as Food Emulsifiers and Stabilizers. *Food Structure*, **12**, 411-426.

42. N. Gladwell, M.J. Grimson, R.R. Rahalkar, P. Richmond (1985). Rheological Behaviour of Soya Oil-in-Water Emulsions: Dependence upon Oil Concentration. *J. Food Sci.*, **50**, 440-443.

43. N. Gladwell, R.R. Rahalkar, P. Richmond (1986). Influence of Disperse Phase Concentration upon the Viscoelastic Behaviour of Emulsion, *Rheol. Acta*, **25**, 55-61.

44. M.Hennock,R.R. Rahalkar, P. Richmond, (1984). Effect of Xanthan Gum upon the Rheology and Stability of Oil-water Emulsions *J. Food Sci.* **49**, 1271-1274.

45. M. Valdes, J. Felix , J.E. Puig (1993). Rheology of Lyotropic Liquid Crystals of Aerosol O.T I.Low Concentration Regime. *J. Coll. Interface Sci.* **160**, 59-64.

46. O.R. Vasquez, S.C. Galvan, J.F.A.Soltero , J.E. Puig (1993). Rheology of Lyotropic Liquid Crystals of Aerosol O.T II.High Concentration Regime. *J. Coll. Interface Sci.* **160**, 65-71.

47. A.M.Orecchioni, G.Couarraze, J.L.Grossiord, F.Puisieux (1984). Viscoelastic Properties of Paracrystalline Phases. *Int. J. of Cosmestic Sci.*,**6**,131-143.

48. S.D. Holdsworth (1993). Rheological Models used for the Prediction of the Flow Properties of Food Products: A Literature Review. Food and Bioproducts Processing. **71(3)**, 139-179.

49. S.G.W Blair (1970). Power Equations Relating Stress to Shear Rate in Rheology. *J. Text. Studies*, **1**, 431-436.

50. J.P. Hartnett & R.Y.Z. Hu. (1989). The Yield Stress-An Engineering Reality. *J. Rheol* **33(4)**, 671-679.

51. A.M.Hermannsson, (1975). Functional Properties of Protein for Foods Flow Properties. *J. Text. Studies*, **5**: 425-439.

52. P.G.Crandall, ,C.S. Chen, , R.D. Carter. (1982). Models for Predicting Viscosity of Orange Juice Concentrate. *Food Technology*, **36(5)**, 245-252.

53. L.G.Rodrigues,J. Segara ,J. Tores, E.Brooi (1987). Heat Transfer to Non-Newtonian Fluid Foods under Laminar Flow Conditions in Horizontal Tubes. *J. Food. Sci.* **52(4)**, 975-979.

54. J.E.B. Wayne, C.F. Shrenks (1988). Rheological Characterization of Commercially Processed Fluid Milks. *J. Text. Studies*,**19**,143-152.

55. E.Costell, E. Carbonell, L.Duran (1987). Chemical Composition and Flow Behaviour of Strawberry Jams - Relation with Fat Content. *Acta Alimentarius*, **16**, 319-220.

56. N.Gladwell, M.J. Grimson,R.R. Rakalkar, P. Richmond (1985c). Rheological Behaviour of Soya Oil-Water Emulsions Dependence upon Oil Concentration, *J. Food Sci.* **50**, 440-3.

57. C.F. Shoemaker (1992). Instrumentation for the Measurement of Viscoelasticity. *Viscoelastic in Properties of Food.* M.A. Rao, J.F. Steffe, Edi., Elsevier, England, 233-246.

58. P. Becher, E.H. Webster (1979). The Effect of Surface Active Agents on the Rheology of Bread and Dough. *Food Texture and Rheology* P. Sherman , Edi. Academic Press, New York, 315-323.

59. N. Gladwell, R.R, Rahalkar, P. Rickmond, (1985a). Creep/Recovery Behaviour of Oil-Water Emulsions: Influence of Disperse Phase Concentration. *J. Food Sci.*, **50**, 1477-81.

60. V.D. Kiosseoglou, P. Sherman (1983). Influence of Egg Yolk Lipoproteins on the Rheology and Stability of O/W Emulsions and Mayonnaise I. Viscoelasticity of Groundnut Oil-in-Water Emulsions and Mayonnaise. *J. Texture Studies*, **14**, 397-417.

61. M.D.C. Parades, M.A. Rao, & M.C. Bourre (1989). Rheological Characterization of Salad Dressings. *J. Texture Studies*, **20**, 235-50.

62. L.R. Correia, (1969). Viscoelastic Properties of Meat Emulsions . *Viscoelastic Properties of Foods.* M.A. Rao,J.F. Steffe,Edi., Elsevier,London, 185-204.

63. J.R. Mitchell (1979). Rheology of Polysaccharide Solutions and Gels. *Polysaccharides in Foods.* J.V.M. Blanshard, J.R. Mitchell Edi. Butterworths, London, 51-72.

64. M. Peleg (1979). Characterisation of the Stress Relaxation Curves of Solids Foods. *J.Food Sci*, **44(1)**, 277-281.

65. F. Shama , P. Sherman (1969). The Influence of Work Softening on the Viscoelastic Properties of Butter and Margarine. *J. Texture Studies*, **1**, 196-205.

66. P. Sherman (1966). The Texture of Ice-Cream 3. Rheological Properties of Mix and Melted Ice-Cream. *J. Food Sci*, **31**, 707-16.

67. G. Schramm (1994). The Measurement of the Elastic Behaviour of Visco-Elastic Fluids. *Gebruedar Haake Gmbh*, , Karlsruhe, Germany,77-126.

68. A. Abdelrahman, A.R. Spies (1986). Dynamic Rheological Studies of Dough Systems. *Fundamentals of Dough Rheology.* H. Faridi, J.M. Faubion, Edi., *Ame. Asso. of Cereal Chem.* St. Paul, U.S.A., 87-103.

69. M.A. Rao (1992). Viscoelastic Properties of Cheeses *Viscoelastic Properties of Foods* M.A. Rao, J.F. Steffe, Edi.,Elsevier, England,173-184.

70. D.D. Hamann (1992). Viscoelastic Properties of Surimi Seafood Products. *Viscoelastic Properties of Foods*. M.A. Rao, J.F. Steffe,Edi., Elsevier, England, 157-172.

71. T.Y. Hung,D.M. Smith (1993) Dynamic Rheological Properties and Microstructure of Partially Insolublised Whey Protein Concentrate Gels. *J. Food Sci.*, **58** (3),1047-49.

72. S.C. Sharma (1979). A Practical Approach to Rheology and Rheometry. Mathematical Modelling of the Viscoelastic Characteritics of Egg York. *J. Food Sci.*, **44**, 1123-1128.

73. R.K.Richardson, S.B.Ross Murphy (1987).Non-linear Viscoelasticity of Polysaccharides Solutions. 1-Guar Galactomannan Solutions. *Int. J. Biol. Macromolecules*, **9**,250-256.

74. A.J.M. Segeren, J.V.Boskamp, M.Van Den Tempel (1974). Rheological and Swelling Properties of Alginate Gels. *Faraday Discuss. Chem.Soc.*, **57**, 255-262.

75. J.H. Elliot, A.J.Ganz (1987). Gel Characterisation with the Weissenberg Rheogoniometer. Application to Carrageenan Gels.*J. Food Sci.*,**40**, 394-398.

76. J.F.A. Soltero, J.E. Puig, O. Manero, P.C. Schulz (1995). Rheology of Cetyltrimethylammonium Tosilate-Water System. I. Relation to Phase Behaviour. *Langmuir*, **11**, 337-3346.

77. J.F.A. Soltero, J.E. Puig, O. Manero (1996). Rheology of the (ethyltrimethylammonium Tosilate-Water System. 2. Linear Viscoelestic Regime. *Langmuir*, **12**, 2654-2662.

78. O.R.Vasquez, J.F.A. Soltero, J.E.Puig, O.Manero (1994). Rheology of Lyotropic Liquid Crystals of Aerosol OT. III. Effects of Salts and Hydrocarbons. *J.Coll. Interface Sci.*,**164**, 432-436.

79. H. Willem, J.L. Boersma, N.s. Hans (1992). Viscoelastic Properties of Concentrated Shear-Thickening Dispersions. *J. Coll. Interface Sci*, **149**, 10-22.

80. W. Liang, Th. F. Tadros, P.F. Luckham (1993). Rheological Properties of Concentrated Sterically Stabilized Latex Dispersions in the Presence of Hydroxyethyl Cellulose. *J. Coll. Interface Sci*, **160**, 183-189.

81. D. Heath and Th.F. Tadros (1983). Influence of pH, Electrolyte and Poly (Vinyl Alcohol). Addition on the Rheological Characteristics of Aqueous Dispersions of Sodium Montmorillonite. *J. Coll. Interface Science*, **93**, 307-319.

82. L.H. Yin, J.J. Yun, M.A. Rao (1993). Rheological Properties of Mozzarella Cheese Filled with Dairy, Egg, Soy Proteins and Gelatin. *J. Food Sci.*, 58**(5)** 1001-1004.

83. G. Stainsby (1991). A Teacher's View. *Food, Polymers, Gels and Colloids* E. Dickinson, Edi., The Royal Soc. of Chem., Cambridge, 450-467.

84. E.E. Braudo, V.B. Tolstoguzov (1983). Fabricated Foodstuffs as Multicomponent Gels. *J. Texture Studies*, **14**, 183-212.

85. Y.Jiang, R.Guo, S.Friberg (1996). The Phase Behaviour of Polyoxyethylene 10 Steryl Ether/Geraniol/Olive oil/Water System and Preliminary Evaluation of Fragrance Evaporation.*Int.J. Cosmetics Sci.*,**18**,43-55.

86. G.Crispulo,B.Manuel (1992). Linear Viscoelastic Behaviour of Commercial and Model Mayonnaise. *J. Rheol.* **26(3)**, 465-478.

87. P.B. Fernandes, M.P. Gonclaves, J.L. Doublier (1993). Influence of Locust Bean Gum on the Rheological Properties of Kappa-Carrageenan Systems in the Vicinity of the Gel Point. *Carbohydrate Polymers*, **22**, 99-106.

88. A.G.Chernik, E.P. Sokolova (1991).A Differential Scanning Calorimetry Study of a Binary System.*J. Coll. Interface Sci.*, **141**, 409-414.

Table 1. Composition of Emuldan

Component	Wt. %*
Glycerol	13.0
Free Fatty Acids	2.1
Monoglycerides	44.1
Diglycerides	36.9
Triglycerides	3.9

* Determined by Gas Chromatography

Table 2. Fatty Acid Composition of Emuldan

Fatty Acid	Wt. %*
C14:0	1.0
C16:0	41.8
C18:0	56.5
C20:0	0.7

*Determined by Gas Chromatography

Table 3: Composition and Appearance of Emulsions prepared using Olein, Emuldan and Water

Sample No.	Emuldan Wt. %	Olein Wt. %	Water Wt. %	Emuldan/ Olein Wt. %	Emuldan/ Water Wt. %	Olein/ Water Wt. %	Appearance
1	3	30	67	10	4.5	44.8	Opaque white, milk-like liquid
2	3	25	72	12	4.2	34.7	"
3	3	20	77	15	3.9	26.0	"
4	3	15	82	20	3.7	18.3	"
5	3	10	87	30	3.4	11.5	"
6	3	5	92	60	3.3	5.4	"
7	5	30	65	17	7.7	46.2	Opaque white creamy liquid
8	5	25	70	20	7.1	35.7	"
9	5	20	75	25	6.7	26.7	"
10	5	15	80	33	6.3	18.8	"
11	5	10	85	50	5.9	11.8	"
12	5	5	90	100	5.6	5.6	"
13	10	30	60	33	16.7	50.0	Opaque white very viscous, non-pourable
14	10	25	65	40	15.4	38.5	"
15	10	20	70	50	14.3	28.6	"
16	10	15	75	67	13.3	20.0	"
17	10	10	80	100	12.5	12.5	"
18	10	5	85	200	11.8	5.9	Opaque white, viscous, pourable
19	15	30	55	50	27.3	54.5	Opaque white, non-pourable solid
20	15	25	60	60	25.0	41.7	"
21	15	20	65	75	23.1	30.8	"
22	15	15	70	100	21.4	21.4	"
23	15	10	75	150	20.0	13.3	"
24	15	5	80	300	18.7	6.3	"

Table 4. Composition and Appearance of Samples Prepared using Water and Emuldan

Sample	Emuldan Wt.%	Water Wt.%	Appearance
A	3	97	Opaque white fluid
B	5	95	Opaque white fluid
C	10	90	Opaque white, viscous, non-pourable
D	15	85	Opaque white, solid
E	20	80	Opaque white, solid
F	25	75	Opaque white, solid
G	30	70	Opaque white, solid

Table 5. Droplet Size Distribution of Sample 1-18,A,B and C

Sample	Droplet Size		Mode of Droplet size Distribution
	Mean Diameter (μm)	Span**	
Emuldan/Water			
A	0.44	1.76	Monomodal
B	0.38	1.00	"
C	0.30	1.01	"
D-G	S	S	S
Emuldan/Water/Oil			
1	2.27	3.35	Bimodal
2	1.70	2.99	"
3	1.18	2.17	"
4	0.75	2.41	"
5	0.41	1.00	Monomodal
6	0.91	1.75	"
7	1.04	1.73	Bimodal
8	0.66	1.70	"
9	0.49	1.38	Monomodal
10	0.40	1.01	"
11	0.41	1.00	"
12	0.62	1.79	"
13	0.51	1.80	Bimodal
14	0.41	1.19	"
15	0.39	1.03	Monomodal
16	0.34	0.71	"
17	0.34	0.80	"
18	0.36	4.20	"
19-24	S	S	S

** Span defined as $\frac{D(V,0.9)-D(V,0.1)}{D(V,0.5)}$ is a measure of the polydispersity of the oil droplets

S - Samples not easily re-dispersable in water

Table 6. Rheological Equations obtained by Curve Fitting of Samples A-B and Samples 1-12. Apparent Viscosities deduced at Shear Rate 30 s^{-1}

Sample	τ_o (Pa)	K	n	χ^{2**}	η_{30} (Pa s)
A	5.25E-02	5.78E-03	5.00E-01	6.68E-09	0.002806
B	9.80E-02	1.25E-01	5.35E-01	2.62E-07	0.028919
1	2.34E-01	1.71E-01	3.53E-01	9.51E-05	0.026794
2	3.90E-01	7.06E-02	2.44E-01	1.50e-04	0.018386
3	4.86E-01	-5.1E-02	2.11E-01	1.05E-04	0.012697
4	3.86E-01	2.38E-04	2.49E-01	3.39E-05	0.012895
5	2.78E-01	1.81E-01	2.75E-01	3.05E-05	0.024694
6	3.42E-01	1.02E-01	2.79E-01	2.77E-05	0.020143
7	2.85E-01	3.56E-01	4.84E-01	2.20E-03	0.07113
8	3.12E-01	1.43E-01	5.04E-01	1.22E-03	0.036907
9	2.85E-01	1.66E-01	4.51E-01	1.10E-03	0.035086
10	5.48E-01	4.03E-02	2.56E-01	3.28E-03	0.021459
11	3.69E-01	1.78E-01	2.55E-01	3.00E-04	0.026387
12	6.13E-01	-1.4E-01	1.82E-01	1.66E-04	0.011466

* Rheological Model of Herschel Bulkley where $\eta_a = \tau_o/\dot{\gamma} + K\dot{\gamma}^{n-1}$ For uniformity the yield value, τ_o, was taken at $\dot{\gamma} = 0.1s^{-1}$ for all the samples.

** The lower the χ^2, the better is the fit. Note extremly low χ^2

Table 7. Steady State Compliance Je_o and Zero Shear Viscosity No of Emuldan / Water and Emuldan/Oil/Water Systems.

Sample	Je_o (Pa^{-1})	No(Pa s)
A-B	N.D	N.D
C	4.894E-03	7.301E+03
D	1.800E-03	3.430E+05
E	1.300E-04	3.360E+06
F	4.5000E-04	1.910E+06
G	4.200E-05	8.220E+06
1-12	N.D.	N.D.
13	2.893E-03	1.663E+05
14	7.812E-03	8.471E+04
15	5.825E-03	1.013E+05
16	1.279E-02	5.232E+04
17	1.441E-01	7.544E+02
18	4.406E-02	5.162E+03
19	1.590E-04	4.478e+06
20	3.155E-04	1.800E+06
21	1.939E-04	1.994E+06
22	1.754E-03	8.449E+05
23	5.754E-04	7.768E+05
24	7.754E-04	8.204E+05

*N.D. Values could not be determined as the lowest stress of the instrument is outside the linear range of the samples. Samples were liquid-like.

Table 8. Rheological Data of Samples C-G and Samples 13-24 at the Critical Stress Value τ_c.

Sample	Emuldan/ Water (W%)	τ_c (Pa)	G* (Pa)	G' (Pa)	G" (Pa)	tan δ
C	10	3.4	121	120	17.2	0.144
D	15	61.1	3870	3830	552	0.144
E	20	200	103000	98700	28600	0.290
F	25	300	86300	82700	24800	0.299
G	30	500	108000	106000	24900	0.235
13	16.7	43.3	1020	1010	136	0.136
14	15.4	23.3	720	713	97	0.136
15	14.3	10.0	453	448	65.1	0.145
16	13.3	11.7	468	466	45.4	0.097
17	12.5	5.0	205	197	55.3	0.280
18	11.8	1.8	19.7	8.84	17.6	2.000
19	27.3	233	44500	43500	9570	0.220
20	25.0	300	73700	71100	19200	0.269
21	23.1	200	33000	32200	7180	0.223
22	21.4	72.2	6130	6060	923	0.152
23	20.0	100	14800	14500	2780	0.192
24	18.7	111	19400	19000	4050	0.214

τ_c, Critical stress value is taken as the stress where there is a gradual change from linearity of the G' as deduced from the respective Moduli vs. Stress sweep data.

Fig. 1. *Structure Models showing (a) Orientation of Surfactant Molecules in the Crystalline stage; b) Formation of lamellar mesophase above Tc (Kraft point) in the presence of water and (c) Formation of gel phase below Tc (d) Hexagonal I, cylindrical aggregates of polar lipids with polar group in contact with the continuous water phase (e) Hexagonal II, cylindrical aggregates of water in a continuous lipid phase.

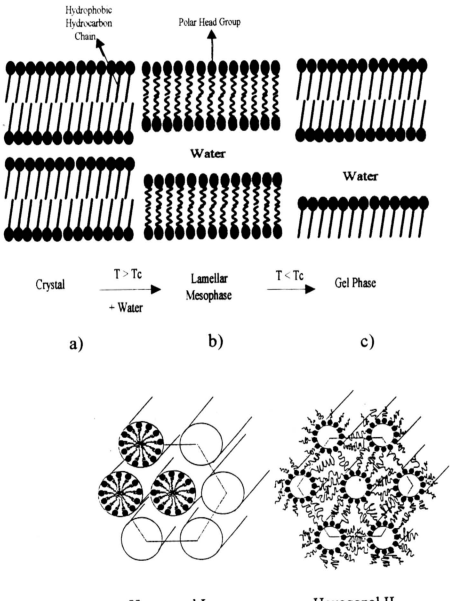

*Reproduced from N. Krog (1990) Food Emulsifiers and their Chemical and Physical Properties. *Food Emulsions* K. Larsson and S.E. Friberg, Ed. Marcel Dekker, New York, 127-180.

Fig. 2. Phase Diagram deduced by Visual Appearance of Samples indicating the Location of the Emulsions Studied.

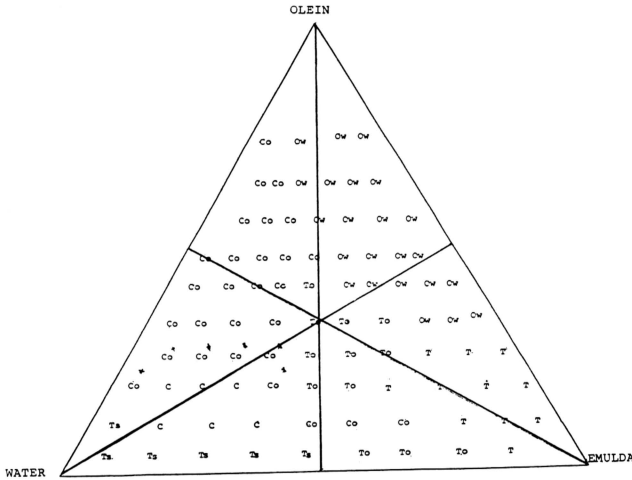

Ow = two layers, slight yellowish turbid oil layer with slightly turbid water layer.

Co*= single phase, creamy white with only a small drop of oil on top

Co = two layers, creamy white layer with yellowish oil on top

To = two layers, clear oil layer on top of turbid water layer

T = single phase, homogenous turbid liquid

Ts = single phase, hard solid

C = single phase, very viscous white cream-like

Fig. 3. Ternary Phase Diagram Indicating the Location of the Samples (1-24) with Respect to the Composition of the Three Components of Emuldan:Olein:Water on Weight Basis.

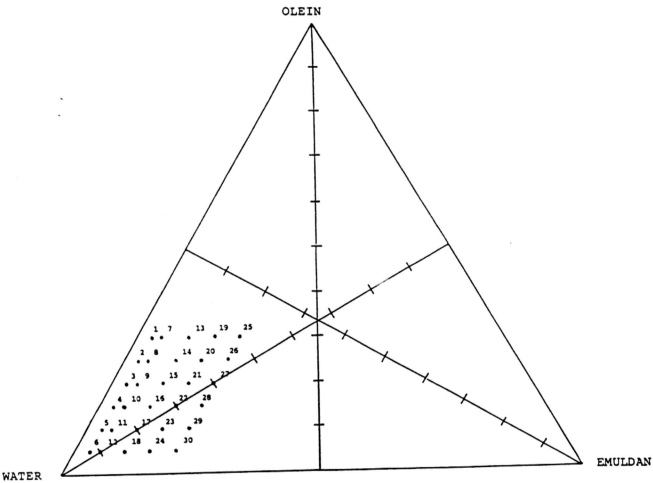

Fig. 4. Visual Observation of Samples A-C and 1-18 after One Week of Storage.

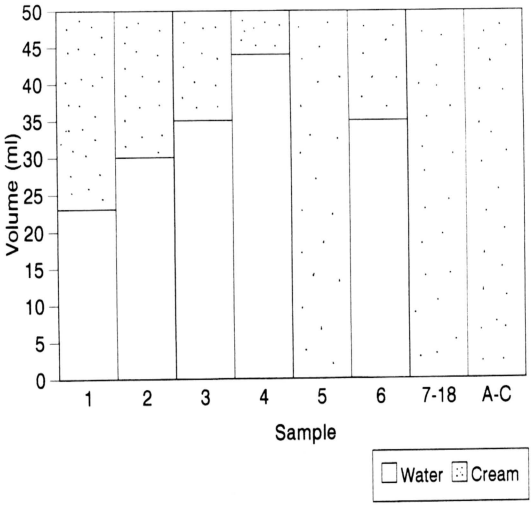

Note: All the samples were opaque white, the dilute aqueous dispersion and top layer of cream demarcation was observed only under intense light.

Fig. 5. Effect of concentration of Emuldan in Olein on the Interfacial Tension of the Olein/Water System at 60°C.

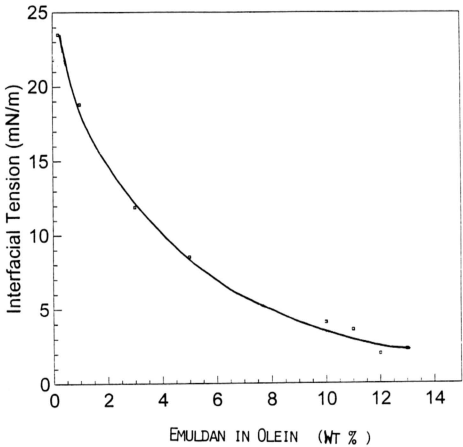

D1
HVKS50S2/M

Fig. 6. Droplet Size Distribution of Emulsion Samples 1-6 and A,B,C.

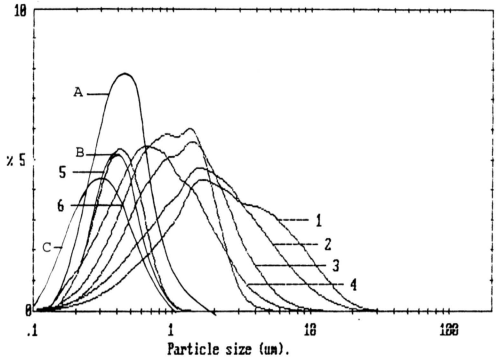

Fig. 7. Droplet Size Distribution of Emulsion Samples 7-12.

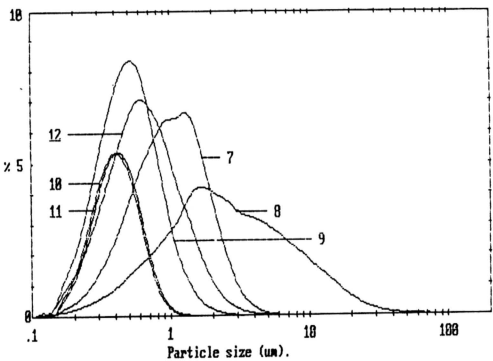

Fig. 8. Droplet Size Distribution of Emulsion Samples 13-18.

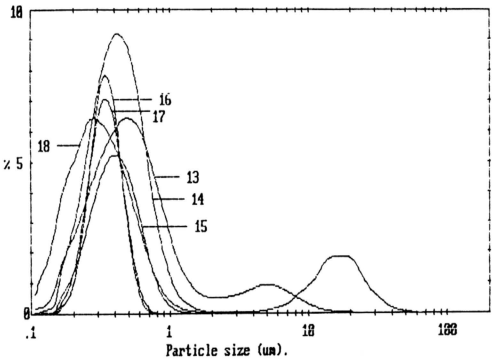

Fig. 9. Mean Droplet Diameter of Emulsions as a Function of Wt. % Emuldan/Water at Various Fixed Concentration of Olein.

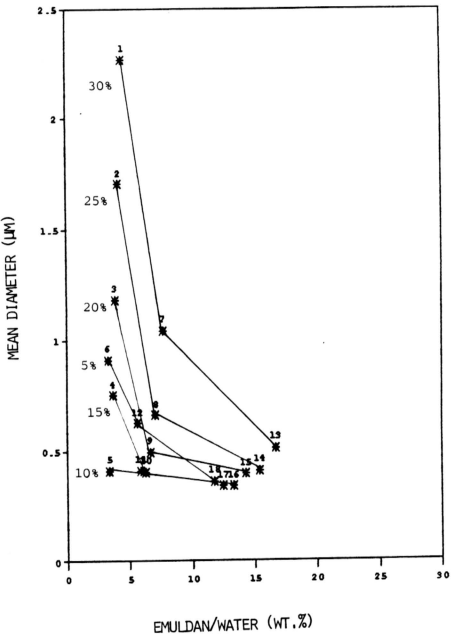

Fig. 10. Mean Droplet Diameter of Emulsions as a Function of Wt.% Olein/Water at Various Concentrations of Emuldan.

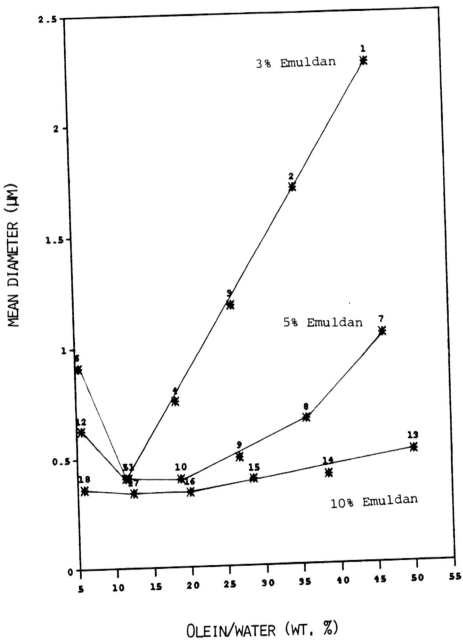

Fig. 11. Mean Droplet Diameter as a Function of Wt.% Emuldan/Oil at Various Concentration of Water. (No systematic correlation among the samples could be determined).

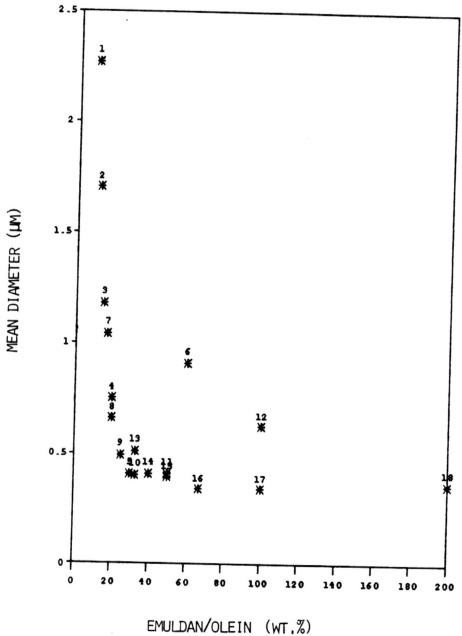

Fig. 12. Optical Micrograph of Sample 2, Containing 3:25:72 (wt.%) of Emuldan:Olein:Water (Mag 10x5).

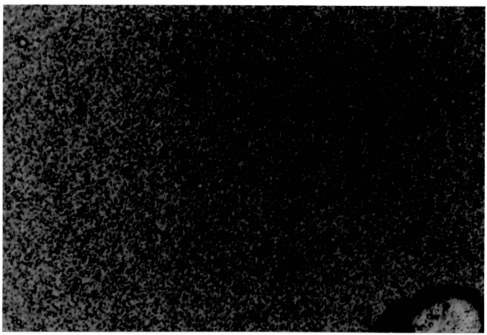

Undiluted Sample

Fig. 13. Optical Micrograph of Sample 5 containing 3:10:87 (wt.%) of Emuldan:Olein:Water. Note the smaller droplets compared to sample 2, Fig. 12 .(Mag 10x5).

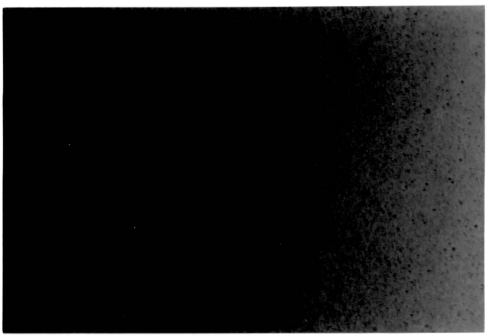

Undiluted Sample

Fig. 14. Optical Micrograph of Sample 13 containing 10:30:60 (wt.%) of Emuldan:Olein:Water. Note aggregation of droplets but well dispersed smaller particles in the background(Mag 10x5).

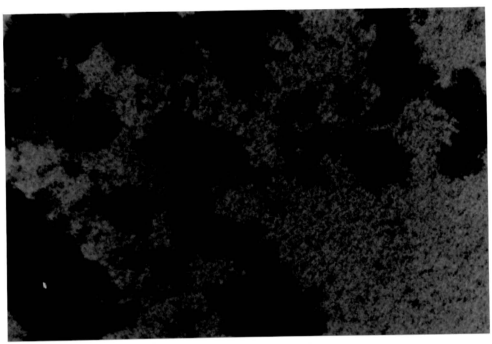

Undiluted Sample

Fig. 15. Optical Micrograph of Sample 20 containing 15:25:60 (wt.%) of Emuldan:Olein:Water. (Mag 10x5).

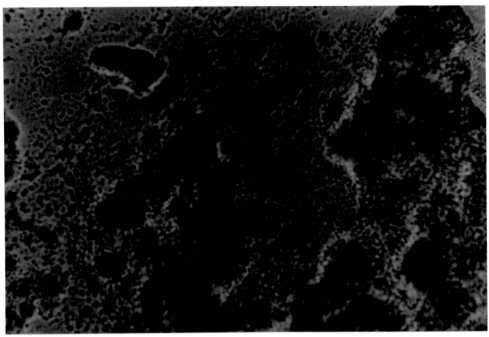

Undiluted Sample

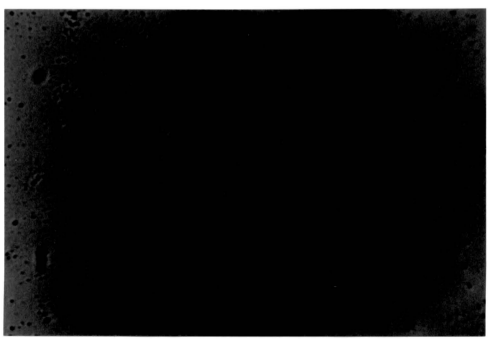

Diluted with Water

Fig. 16. Optical Micrograph Showing Crystals Formation after Three Weeks Storage ofSample10containing 5:15:80 (wt.%) of (Emuldan:Olein:Water). Note well dispersed smaller particles in the background.(Mag.10x5)

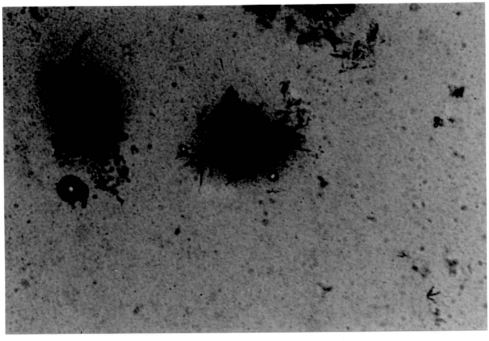

Fig. 17. Optical Micrograph of Sample 9 containing 5:20:75 (wt.%) of Emuldan:Olein:Water stored for 6 months (Mag.10x5)

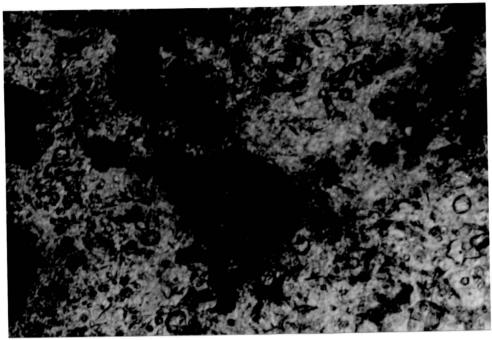

Unpolarised Light

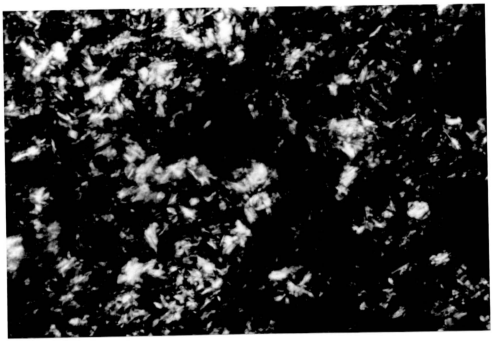

Polarised Light

Fig. 18. Optical Micrograph of Dispersions Formed with 5 Wt.% Emuldan in Water, showing Birefringent Droplets will Extinction Crosses under Polarised Light.

Mag. (5X10)

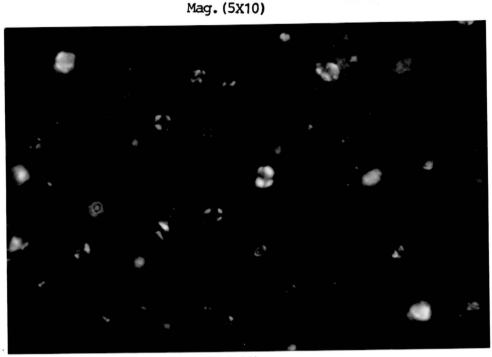

Mag. (5X40)

Fig. 20. Optical Micrograph of Lamellar Liquid Crystalline Structures in Sample E containing 20 Wt. % Emuldan in Water (Mag. 10x5).

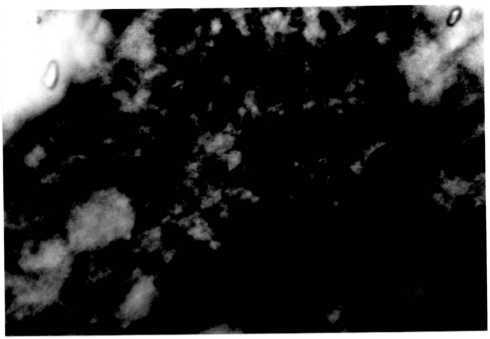

Unpolarised Light

Polarised Light

Fig. 21. Flow Curves of Samples A,B and 1-12 as illustrated by Samples A,B , 7 and 11 (Flow curves of the rest of the samples are very close and thus not shown).

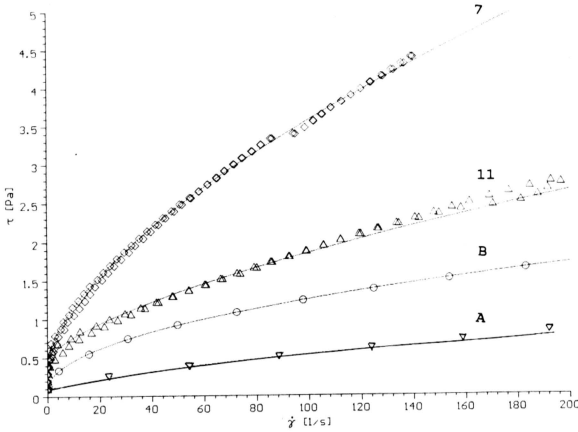

Symbols represent experimental data. Solid lines are Herschel Bulkley model fit where $\tau = \tau_o + K\dot{\gamma}^n$ at $\dot{\gamma}$ 0.1-100s^{-1}. The yield stress τ_o is taken at $\dot{\gamma}$= 0.1s-1

Fig. 22. *Viscosity Curves of Samples A,B and 1-12 as illustrated by Samples A,B, 7 and 11. Flow curves of the rest of the samples are very close and thus are not shown.

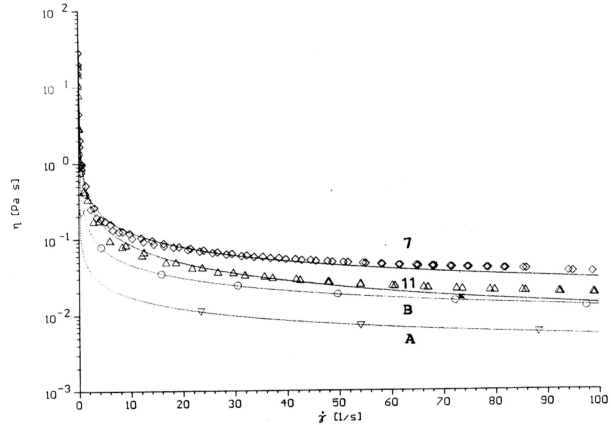

*Symbols represent experimental data. Solid lines are Herschel Bulkley model fit. where $\eta = \tau_o/\gamma + K\dot{\gamma}^{n-1}$ at γ 0.1-100s^{-1}. The yield stress τ_o is taken at $\dot{\gamma}$= 0.1s^{-1}

Fig. 23. *Apparent Viscosity at Shear Rate $\dot{\gamma}$, $30s^{-1}$ against Wt.% Emuldan in Water for Samples A,B and 1-12.

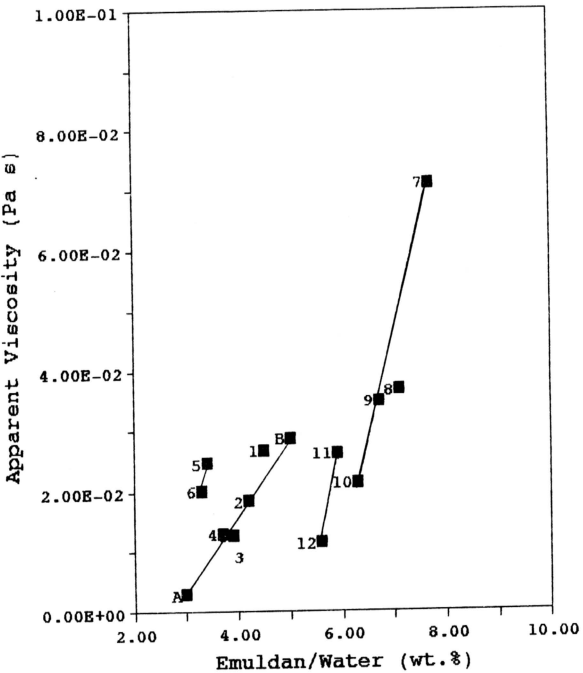

*Apparent viscosity as calculated using the Herschel-Bulkley model where $\dot{\gamma} = 30s^{-1}$

Fig. 24. Illustrative Creep-Recovery Curve of a Viscoelastic Material

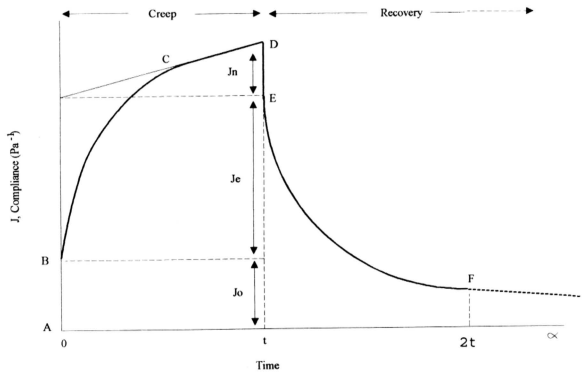

Adapted from : M.A. Rao (1992) Measurement of Viscoelastic Porperties of Fluid and Semi Solid Foods Viscoelastic Properties Of Foods. Ed. M.A.Rao & J.F. Steffe, Pub. Elsevier App. Sci, U.S.A., 221.

Fig. 25. * Creep Recovery Curve of Samples C-G

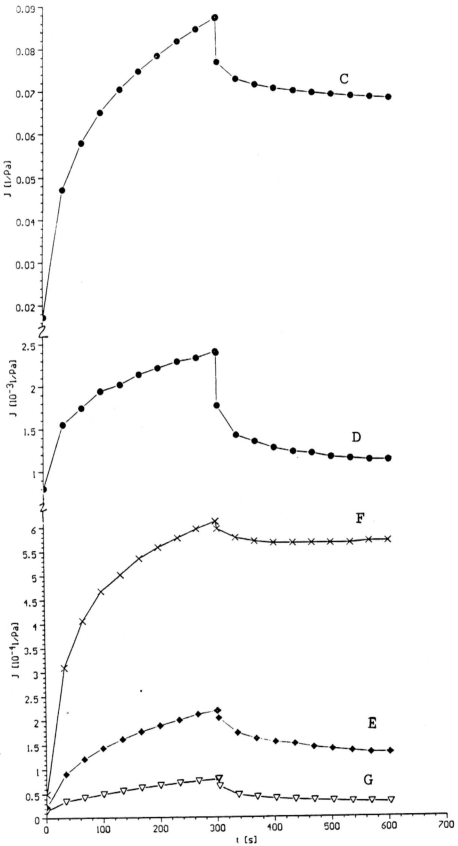

* Note different Y-axis

Fig. 26. Creep Recovery Curves of Samples 13-24 as illustrated by Samples 13 , 16 and 23.

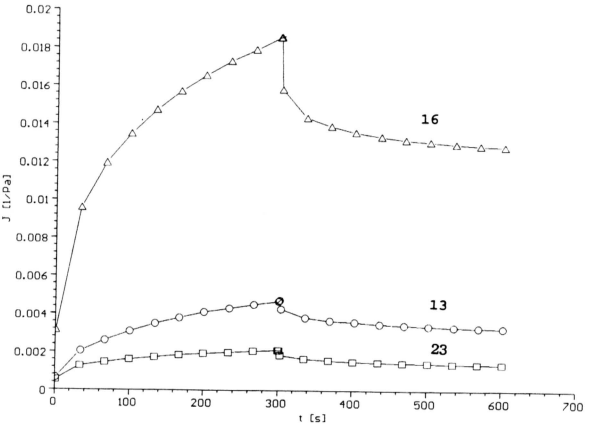

Fig. 27. A Plot of Steady State Compliance J_e^o of Samples 13-24 and C-G as a Function of Wt.% Emuldan/Water.

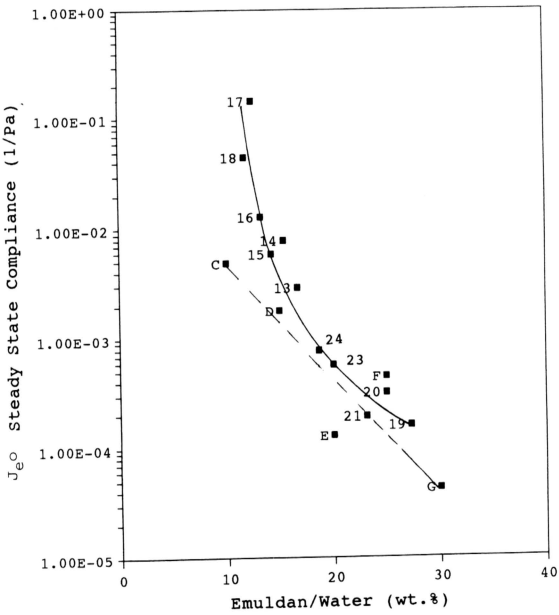

Fig. 28. A Plot of Zero Shear Viscosity, η_o for Samples C-G and 13-24 as a Function of Wt.% Emuldan/Water.

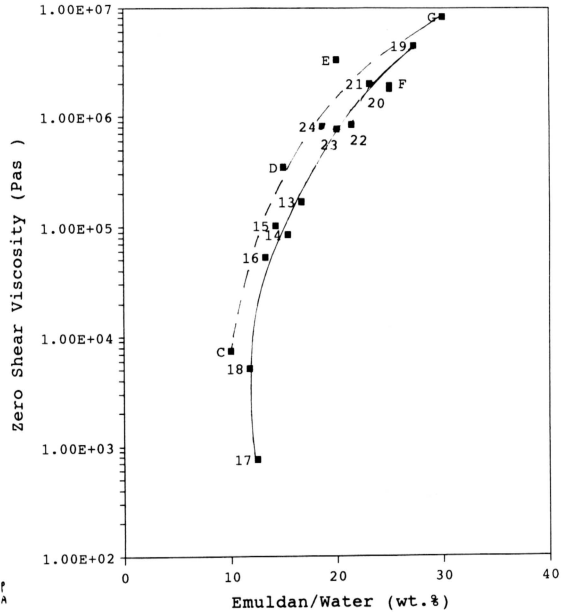

Oil
File:Creep
Graph 31A

Fig.29. Illustrative Shear Stress Response of a Viscoelastic Material. The shift angle δ is a Measure of the Degree of Viscoelasticity of the Material.

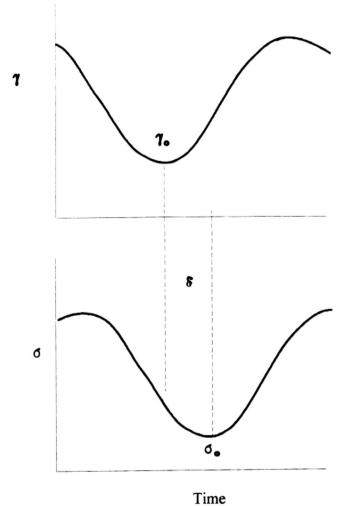

Adapted from : C. F. Shoemaker (1992) Instrumentation for The Measurement of Viscoelasticity, Viscoelastic Properties of Foods, Ed. M.A.Rao & J.F. Steffe. Pub. Elsevier App. Sci. U.S.A, 243.

Fig. 30. Stress Sweep of Samples C-G at 1 Hz. Note G* overlaps G'. Inset shows the stress sweep overlap of samples E-G.

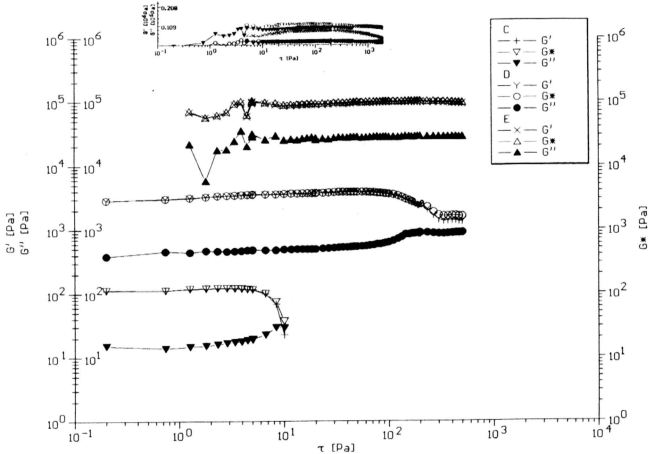

Fig. 31. Plot of G′ and G″ as a Function of Wt.% of Emuldan/Water at the Linear Viscoelastic Region (Note G′ > G″)

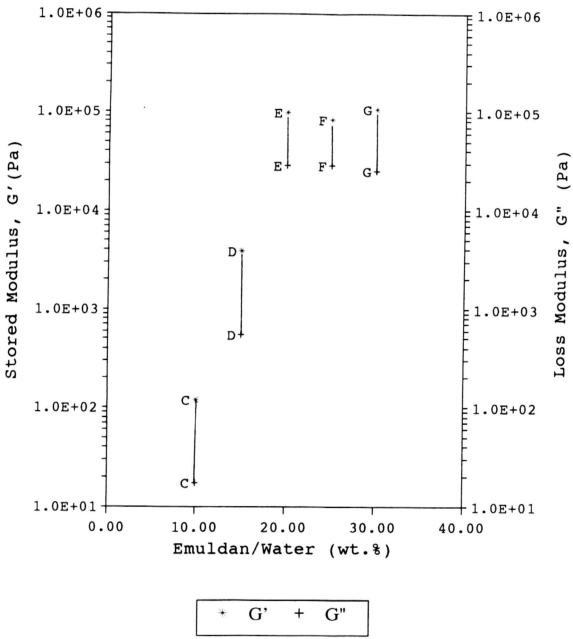

Fig. 32. Typical Stress Sweep of Samples 13-18 at 1 Hz. as illustrated by Samples 14,17 and 18. Note G* overlaps G' except sample 18.

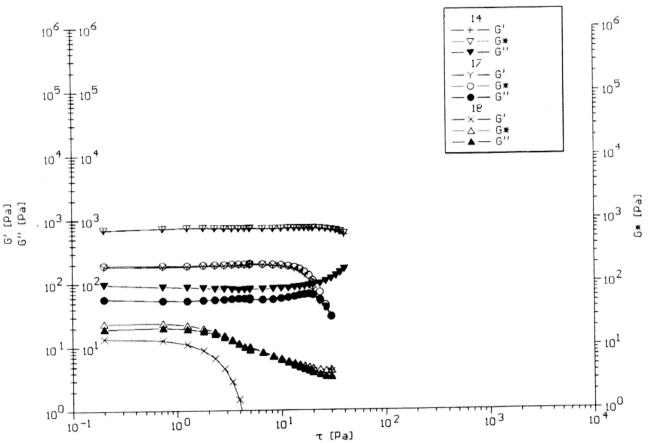

Fig. 33. Plot of G', G" as a Function of Wt.% Emuldan/Water at the Linear Viscoelastic Region .
(Note G'>G" except sample 18).

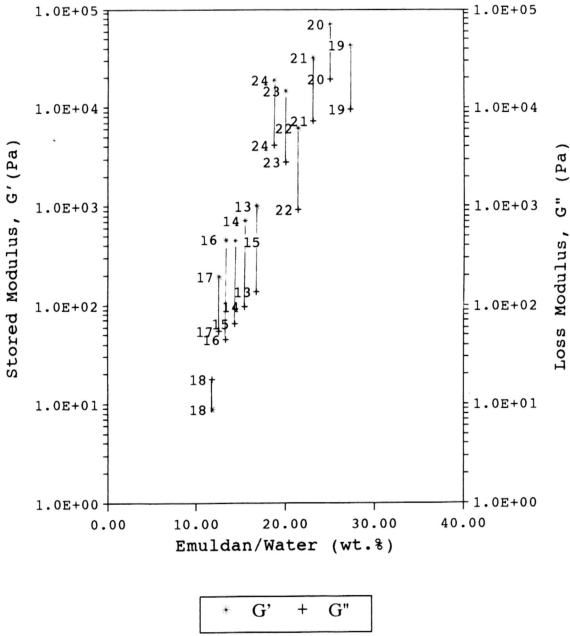

RI
Rheo
13-24 G G"

Fig. 34. Typical Stress Sweep of Samples 18-24 at 1Hz as illustrated by Samples 20,21 and 23. Note G* overlaps G'.

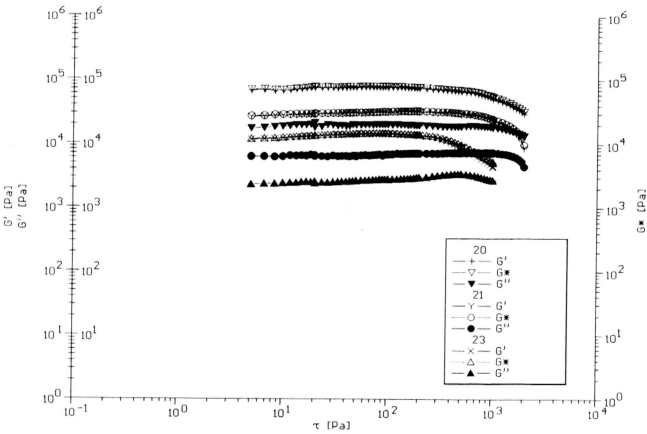

Fig. 35. Plot of Critical Stress of Samples C-G, 13-24 as a Function of Wt.% Emuldan/Water.

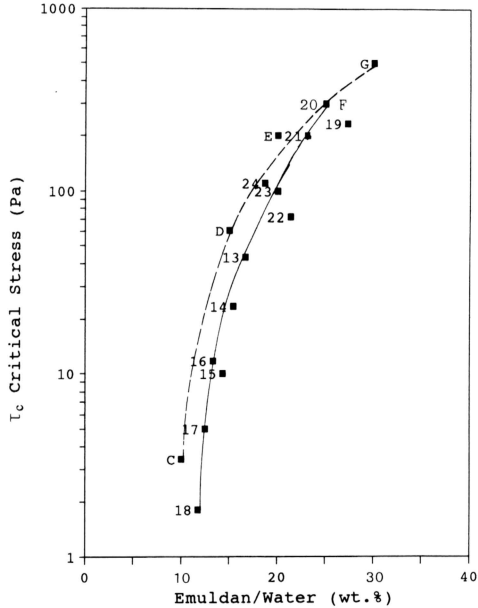

Fig.36. Plot of G' at T_c as a Function of Wt.% Emuldan/Water illustrating the Decrease in G' in the Ternary System (Samples 13-24) as compared to the Binary System (Samples C-G).

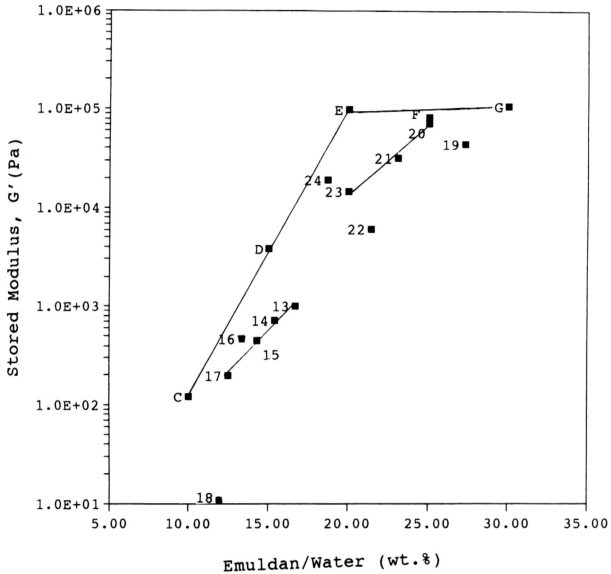

Fig. 37. Frequency Sweep of Samples C-G at 20 Pa. Note G* overlaps G'. Inset shows the Frequency Sweep Overlap of Samples E-G.

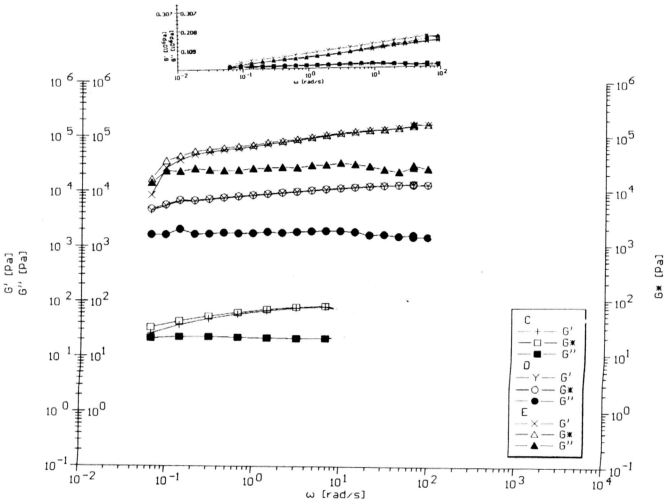

Fig. 38. Typical Mechanical Spectra of Samples 13-18 at 5 Pa as illustrated by Samples 13, 15, 17 and 18. Note overlap of G* and G'.

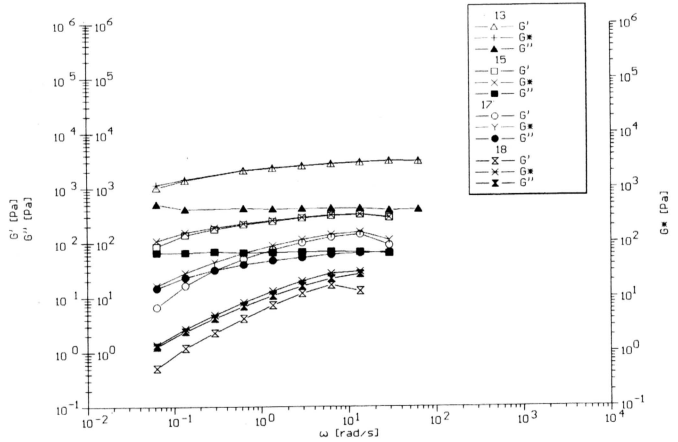

Fig. 39. Typical Mechanical Spectra of Samples 19-24 at 20 Pa as illustrated by Samples 19,20 and 23. Note overlap of G* and G'.